NATIONAL ADVISORY COMMITTEE FOR AERONAUTICS

TECHNICAL NOTE 2747

CHARTS AND APPROXIMATE FORMULAS FOR THE ESTIMATION OF AEROELASTIC EFFECTS ON THE LATERAL CONTROL OF SWEPT AND UNSWEPT WINGS

By Kenneth A. Foss and Franklin W. Diederich

Langley Aeronautical Laboratory
Langley Field, Va.

Washington

July 1952

CONTENTS

NATIONAL ADVISORY COMMITTEE FOR AERONAUTICS

TECHNICAL NOTE 2747

CHARTS AND APPROXIMATE FORMULAS FOR THE ESTIMATION OF AEROELASTIC EFFECTS ON THE LATERAL CONTROL OF SWEPT AND UNSWEPT WINGS

By Kenneth A. Foss and Franklin W. Diederich

SUMMARY

Charts and approximate formulas are presented for the estimation of static aeroelastic effects on the spanwise lift distribution, rolling-moment coefficient, and rate of roll due to the deflection of ailerons on swept and unswept wings at subsonic and supersonic speeds. Two types of stiffness distributions are considered, one which consists of a variation of stiffness with the fourth power of the chord and one which is based on an idealized constant-stress structure. Some design considerations brought out by the results of this paper are discussed. This paper treats the lateral-control case in a manner similar to that employed in NACA TN 2608 for the symmetric-flight case and is intended to be used in conjunction with NACA TN 2608 and the charts and formulas presented therein.

INTRODUCTION

The lateral control and maneuverability of a wing are important design considerations. These characteristics may be affected to a significant extent by aeroelastic action, particularly at high dynamic pressures and in the case of thin wings, swept wings, and wings designed for low wing loadings, because the operation of ailerons and spoilers usually creates aerodynamic forces which deform the wing.

As a result of these deformations, the angles of attack along the span often change in such a manner as to produce lifts which oppose the rolling moment of the aileron or spoiler; furthermore, these lifts cause additional deformations which may again reduce the rolling moment, and so on, until equilibrium is reached. Wing flexibility may thus cause a serious loss in the control power; in fact, if the dynamic pressure of the air stream is sufficiently high, the aileron rolling moment may be completely nullified. The speed and dynamic pressure at this condition are often referred to as the aileron reversal speed and reversal

dynamic pressure, because at higher dynamic pressures the controls would have to be reversed in order to roll the airplane. When wing flexibility causes a loss in lateral control, there is also usually a loss in the rolling maneuverability, which may be expressed as the wing-tip helix angle due to rolling and is affected by changes in both the control power and the damping in roll. These aeroelastic effects on the lateral control and maneuverability have to be taken into account in the design of a wing.

Several methods are available for calculating these effects (reference 1, for instance), but since these effects depend on the structural characteristics of the wing, which are not accurately known in advance of its design, the relatively large amount of time required for even the most efficient of these methods militates against their use in connection with preliminary design calculations. A need exists, therefore, for means of estimating some of the more important aeroelastic effects on lateral control quickly with an accuracy that is sufficient for preliminary design purposes.

The related problem of estimating static aeroelastic effects on the magnitude and spanwise distribution of the lift in symmetric flight has been treated by the charts and approximate formulas presented in reference 2. The present paper consists of an extension of the analysis of reference 2 to the lateral-control case. Inasmuch as the static aeroelastic equations are linear, the results presented in the two papers may be superimposed. Included in the present paper are approximate formulas for the estimation of the static aeroelastic effects on the spanwise lift distribution, rolling moment, and rate of roll due to aileron deflections on swept and unswept wings at subsonic and supersonic speeds. Also presented are summary charts which indicate whether a given design is likely to be affected by losses in lateral control. By means of these charts and approximate formulas as well as those of reference 2, the conventional procedure of designing a wing on the basis of certain strength criteria, checking it for aeroelastic phenomena, and then reinforcing it, when necessary, to meet the stiffness requirements imposed by these phenomena can often be simplified greatly inasmuch as the effect of some of these phenomena can be estimated in advance of design.

In order to keep the length of the paper to a minimum and to avoid a repetition of much of the material presented in reference 2, the present paper has been written in such a manner as to facilitate its joint use with reference 2 rather than to make it entirely self-contained. The use of the charts and approximate formulas presented herein is described and the limitations of the charts and the light they shed on some design problems are discussed. A numerical example is included to illustrate the use of the approximate formulas of this paper. A brief description of the calculations (based on references 1 and 2) on which

the charts and approximate formulas are based is contained in the appendix to supplement the more detailed derivations in references 1 and 2.

SYMBOLS

A	aspect ratio (b^2/S)
A_Λ	swept-span aspect ratio $(A/\cos^2\Lambda)$
a	location of section aerodynamic center measured from leading edge, fraction of chord
b	wing span, inches
c	chord (measured perpendicular to elastic axis), inches
c_a	aileron chord, inches
c_{l_α}	section lift-curve slope per radian
$C_{L_{\alpha_e}}$	effective wing lift-curve slope per radian
C_l	rolling-moment coefficient
C_{l_p}	damping-in-roll derivative
C_{l_δ}	rolling-moment coefficient due to aileron deflection
cp_δ	location of chordwise center of pressure of lift produced by aileron deflection measured from leading edge, fraction of chord
d	dimensionless sweep parameter $\left(\frac{(GJ)_r}{(EI)_r}\tan^2\Lambda\right)$
E	Young's modulus of elasticity, pounds per square inch
e	location of elastic axis measured from leading edge, fraction of chord
e_1	dimensionless moment arm of section lift about elastic axis $(e - a)$

e_2 dimensionless moment arm of lift due to aileron deflection about elastic axis $(cp_\delta - e)$

F_r root-stiffness function given in reference 2, equation (B25)

F_B allowable bending stress, pounds per square inch

f_a dimensionless function of distance along span used in approximate formulas for angle of attack due to aeroelastic action of ailerons

G modulus of rigidity, pounds per square inch

h wing thickness, inches

I section bending moment of inertia, inches^4

$\bar{I}$ mass moment of inertia of entire airplane about its longitudinal axis, inches^4

$\bar{I}_w$ mass moment of inertia of both wings about longitudinal axis of airplane, inches^4

J section twisting moment of inertia, inches^4

$K_1, K_2, \ldots K_7$ dimensionless parameters used in approximate formulas for dimensionless dynamic pressures at aileron reversal given in table I

k dimensionless sweep parameter $\left(\frac{s_t}{e_1 c_r} \frac{(GJ)_r}{(EI)_r} \tan \Lambda\right)$; the dimensionless parameter k/ϵ is identical to k except that e_1 is replaced by e_2

l lift per unit distance along span, pounds per inch

L'_w rolling moment on both wings, inch-pounds

M bending moment about an axis perpendicular to elastic axis, inch-pounds

M_o free-stream Mach number

n design load factor

$\dot{p}$ rolling acceleration, radians per second per second

$pb/2V$ wing-tip helix angle due to roll, radians

q dynamic pressure, pounds per square foot

q^* dimensionless dynamic pressure $\left(\frac{q}{144}\frac{C_{L_{\alpha_e}} e_1 c_r^2 s_t^2 \cos \Lambda}{(GJ)_r}\right)$; the dimensionless dynamic pressure ϵq^* is identical to q^* except that e_1 is replaced by e_2

$\bar{q}$ dimensionless dynamic pressure $\left(\frac{q}{144}\frac{C_{L_{\alpha_e}} c_r s_t^3 \sin \Lambda}{(EI)_r}\right)$

S total wing area, square inches

s distance along elastic axis measured from wing root, inches

s^* dimensionless distance along elastic axis (s/s_t)

T accumulated torque about elastic axis, inch-pounds

t_i distributed torque due to inertia loading, inch-pounds per inch

V airspeed, feet per second

W design gross weight of airplane, pounds

W_s weight of primary structure of both wings, pounds

y lateral coordinate, inches

α angle of attack in planes parallel to plane of symmetry, radians

α_δ angle of attack equivalent to unit aileron deflection, radians

Γ angle of local dihedral, radians, or spanwise slope of normal displacement of elastic axis

δ aileron deflection measured in planes parallel to air stream, radians

ϵ	moment-arm ratio (e_2/e_1)
$\eta_a,\eta_b,\eta_1,\cdots\eta_{21}$	structural-effectiveness factors defined in equations (15) and table 1 of reference 2
Λ	angle of sweepback at elastic axis
λ	wing taper ratio (c_t/c_r)
ρ	density, slugs per cubic foot
φ	angle of structural twist in planes perpendicular to elastic axis, radians
ω	tip-stiffness-ratio parameter $\left(\frac{(EI)_t}{(EI)_{t_{\text{constant stress}}}}\right)$
1_a	unit step function of distance along span

Subscripts:

D	at divergence
i	at inboard end of aileron; inertia, in equation (36b)
R	at aileron reversal
r	at wing root
s	structural (due to structural deformation)
t	at wing tip
0	rigid wing (for $q^* = \epsilon q^* = \bar{q} = 0$)

USE OF THE CHARTS AND APPROXIMATE FORMULAS

Summary of Method and Scope of the Calculations on Which the Charts and Approximate Formulas Are Based

A brief description of the method and scope of the calculations is given here to indicate the limitations of the charts and approximate formulas. A detailed description of the method is given in the appendix.

Most of these calculations were performed by an extension, based on reference 1, of the matrix method of reference 2. This method consists in solving the differential equations descriptive of an elastically deformed wing under aerodynamic loadings by numerical methods employing matrix techniques. Treated by this method were wings with three taper ratios (1, 0.5, 0.2), one aileron span, two types of stiffness distributions, several values of the sweep parameters k and d which include sweptforward, unswept, and sweptback wings, and several values of the section moment-arm ratio ϵ and the dynamic-pressure ratio q/q_D. Calculated for each case were the dynamic pressure at aileron reversal and the changes in the spanwise lift distribution and rolling moment due to aileron deflection. For the constant-chord, constant-stiffness wings calculations were also performed by an extension of the analytic method of reference 2, which consists in solving the differential equations exactly for these relatively simple cases. These calculations were made for two aileron spans and several values of the parameters k, d, ϵ, and q/q_D.

Two important approximations that have been made in all calculations are as follows:

(1) Aerodynamic induction effects at subsonic speeds are taken into account by an over-all reduction and, in most of the calculations, by rounding off the strip-theory loading at the tip and at the inboard end of the aileron in a manner described in the appendix; at supersonic speeds strip theory is used, with a small reduction at the tip in the matrix calculations

(2) The rigid-body rotations imparted to a swept wing by its triangular root portion are taken into account by a suitable choice of an effective root

These assumptions were made to reduce the number of independent parameters and to make the results more generally applicable. The most severe limitation on the use of the charts is probably imposed by the fact that calculations have been made for only two types of stiffnesses:

(1) Stiffness distributions which vary as the fourth power of the chord, such as those of solid wings

(2) Stiffness distributions associated with structures designed for a constant level of combined bending and torsion stress at every point on the span

Except for solid wings and those with geometrically similar cross sections, for which the stiffnesses vary as the fourth power of the chord, the stiffness distributions of any given wing depend on the detailed design of the wing and cannot be generalized easily. Consequently,

the constant-stress concept, which is discussed in detail in appendix B of reference 2, has been used to estimate stiffness distributions for some of the calculations. This concept constitutes an effort to relate the stiffness of a wing to its strength on the basis of the following assumptions:

(1) The combined bending and torsional stresses are constant along the span

(2) The bending and torsional stresses are combined in such a manner that the sum of the ratio of the actual to the allowable bending stress and the ratio of the actual to the allowable torsion stress is equal to unity when the margin of safety is zero

(3) The structure is of the thin-skin, stringer-reinforced shell type and its main features do not vary along the span; for instance, the number of spars and their chordwise locations are constant along the span

(4) At the design condition the spanwise distribution of the applied loading is proportional to the chord

Selection of Parameters

Geometric parameters.- The geometric parameters used in the analysis are defined in figure 1. The location of the effective root indicated in this figure is discussed in reference 2. In the present paper the angle of aileron deflection δ is defined as being measured in planes parallel to the air stream. This angle is equal to the product of the angle of rotation of the aileron about the hinge axis and the cosine of the sweep angle of the hinge axis.

Although most of the charts and approximate formulas are based on a half-span outboard aileron ($s^*_i = 0.5$), the results of the analysis of the uniform wings with full-span ailerons ($s^*_i = 0$) and "tip ailerons" ($s^*_i \rightarrow 1$) indicate that, except for the angle-of-attack distributions, the results based on a half-span aileron may be expected to be valid for outboard ailerons having spans which differ considerably from one-half.

Aerodynamic parameters.- The aerodynamic parameters which enter the analysis are the effective wing lift-curve slope, the location of the wing aerodynamic center, the location of the chordwise center of pressure due to aileron deflection, and the angle of attack equivalent to unit aileron deflection. An effective wing lift-curve slope $C_{L_{\alpha_e}}$, applicable to basic lift distributions due to built-in twist, aileron deflection, roll, or aeroelastic twist, is approximately given by the relation

$$C_{L_{\alpha_e}} = c_{l_\alpha} \frac{A \cos \Lambda}{A + 4 \frac{c_{l_\alpha}}{2\pi} \cos \Lambda} \tag{1}$$

at subsonic speeds, where c_{l_α} is approximately given by

$$c_{l_\alpha} = \frac{2\pi}{\sqrt{1 - M_o^2 \cos^2 \Lambda}} \tag{2}$$

The basis of equation (1) is explained in reference 2. At supersonic speeds the effective wing lift-curve slope is approximately

$$C_{L_{\alpha_e}} = \frac{4 \cos \Lambda}{\sqrt{M_o^2 \cos^2 \Lambda - 1}} \tag{3}$$

provided M_o is greater than $1/\cos \Lambda$. If M_o is greater than 1 but less than and not too close to $1/\cos \Lambda$, equations (1) and (2) may be used in the absence of better information; however, the results obtained for this range of Mach numbers should be used with caution.

The lift-curve slopes given by equations (1) and (3) should not be confused with the rigid-wing lift-curve slope or the damping-in-roll derivative; they are merely effective values suitable for aeroelastic calculations. Values of the rigid-wing lift-curve slope and the damping-in-roll derivative can be used in conjunction with the methods of the present paper and of reference 2 to obtain the values of the flexible-wing lift-curve slope and the damping-in-roll derivative because means are presented herein and in reference 2 for estimating the ratios of the flexible-wing to the rigid-wing values. For this purpose any experimental information concerning the rigid-wing values can be used; if none is available references 3, 4, and 5 may be used at supersonic speeds and reference 6, at subsonic speeds.

The local aerodynamic centers are assumed to be at a constant fraction of the chord from the leading edge, so that they are all equal to the wing aerodynamic center as a fraction of the mean aerodynamic chord. The moment arm e_1 is then given by the relation

$$e_1 = e - a \tag{4}$$

The local centers of pressure of the lift due to aileron deflection are also assumed to be a constant fraction of the chord from the leading edge; and the moment arm e_2 is then given by

$$e_2 = cp_\delta - e \tag{5}$$

Theoretical two-dimensional values of the parameter cp_δ are presented in figure 2 for both trailing-edge and leading-edge ailerons at subsonic and supersonic speeds. At subsonic speeds the effect of finite span is to shift the center of pressure rearward. An appropriate value for this rearward shift may be estimated from the following relation, based on lifting-line theory for unswept elliptic wings with full-span ailerons:

$$cp_{\delta_{III}} - cp_{\delta_{II}} = \frac{4}{A}\left(cp_{\delta_{II}} - \frac{1}{4}\right)$$

where the subscripts II and III refer, respectively, to two- and three-dimensional values. The use of the swept-span aspect ratio in place of A should serve to extend this approximate relation to swept wings.

Theoretical two-dimensional values of α_δ, the angle of attack equivalent to unit aileron deflection, are also given in figure 2. At low aspect ratios the values of α_δ for subsonic speeds tend to be higher than these two-dimensional values; as the aspect ratio approaches 0, α_δ approaches 1, at least in the case of wings without reentrant trailing edges. Experimental values of both α_δ and cp_δ are preferable to theoretical values if they are available. For spoilers these values always have to be obtained experimentally.

The effective lift-curve slope and the values of the section moment arms vary with the free-stream Mach number; hence, the appropriate values must be used at each flight condition for which aeroelastic calculations are made.

The airspeeds at which the lateral-control aeroelastic phenomena are of interest enter the calculations in the form of the corresponding dynamic pressures. These dynamic pressures, in turn, are expressed in dimensionless form by means of the relations

$$q^* = \frac{q}{144}\frac{C_{L_{\alpha_e}} e_1 c_r^2 s_t^2 \cos \Lambda}{(GJ)_r} \tag{6}$$

$$\epsilon q^* = \frac{q}{144} \frac{C_{L_{\alpha_e}} e_2 c_r^2 s_t^2 \cos \Lambda}{(GJ)_r} \tag{7}$$

or

$$\bar{q} = \frac{q}{144} \frac{C_{L_{\alpha_e}} c_r s_t^3 \sin \Lambda}{(EI)_r} \tag{8}$$

The ratios of these quantities,

$$k = \frac{\bar{q}}{q^*} = \frac{s_t}{e_1 c_r} \frac{(GJ)_r}{(EI)_r} \tan \Lambda \tag{9}$$

and

$$\frac{k}{\epsilon} = \frac{\bar{q}}{\epsilon q^*} = \frac{s_t}{e_2 c_r} \frac{(GJ)_r}{(EI)_r} \tan \Lambda \tag{10}$$

are independent of the dynamic pressure and are very useful for analyzing the aeroelastic behavior of swept wings. Two other dimensionless parameters, which are independent of the dynamic pressure, enter the calculations:

$$\epsilon = \frac{e_2}{e_1} \tag{11}$$

and

$$d = \frac{(GJ)_r}{(EI)_r} \tan^2 \Lambda \tag{12}$$

Structural parameters.- For the purposes of an aeroelastic analysis the wing structure is characterized by the location of the elastic axis, the magnitude and distribution of the bending and torsional

stiffnesses EI and GJ, and the magnitude of the rigid-body rotations imparted to the wing by its root (taken into account in this paper only by the location of an effective root). The selection of these structural parameters is discussed fully in reference 2.

Preliminary Survey of Loss in Lateral Control

The information contained in some of the charts and approximate formulas presented in the following sections of this paper has been summarized in figures 3 to 5 for the purpose of ascertaining in advance of more detailed estimates, if desired, whether the aeroelastic phenomena considered in this paper are likely to affect the design of the wing structure. This preliminary survey is not essential to any of the further calculations but may show them to be unnecessary in some cases. These figures pertain to constant-stress wings with half-span outboard ailerons.

The charts of figures 3(a), 4(a), and 5(a) pertain to wings of taper ratios 0.2, 0.5, and 1.0, respectively, with the moment arm e_2 equal to 0 (corresponding roughly to subsonic flow conditions and elastic-axis locations fairly far back on the wing). These figures show the dynamic-pressure parameter q^* defined by either equation (6) or

$$q^* = \frac{(1+\lambda)^2}{18432} \frac{C_{L_{\alpha_e}} e_1 \cos \Lambda}{\frac{G}{F_B} \frac{nW}{S} \frac{h_r}{c_r} F_r \eta_a} q \tag{13}$$

plotted against the sweep parameter k defined by equation (9) or

$$k = \frac{1+\lambda}{2} \frac{G}{E} \eta_b \frac{A_\Lambda}{\eta_{19} e_1} \tan \Lambda \tag{14}$$

for several values of the aileron effectiveness parameter $C_{l_\delta}/C_{l_{\delta_0}}$ and for two values of the stiffness parameter

$$\frac{d}{k^2} = \frac{(EI)_r}{(GJ)_r} \left(\frac{e_1 c_r}{s_t} \right)^2 \tag{15}$$

or

$$\frac{d}{k^2} = \frac{32}{(1+\lambda)^2}\frac{E}{G}\left(\frac{\eta_{19}e_1}{A_\Lambda}\right)^2 \frac{\eta_6{\eta_7}^2}{\eta_8\eta_9\eta_{15}{\eta_b}^2} \tag{16}$$

where F_r is a root-stiffness parameter defined and given in reference 2 and where the structural-effectiveness factors η_a, η_b, η_6, η_7, η_8, η_9, η_{15}, and η_{19} are also defined in reference 2. (If, at the time a preliminary survey of aeroelastic effects is to be made, no information whatever concerning the wing stiffness is available, equations (13), (14), and (16) may be used; if an estimate of the root stiffnesses $(GJ)_r$ and $(EI)_r$ is available, equations (6), (9), and (15) may be used.)

The charts of figures 3(b), 4(b), and 5(b) are the same as those of figures 3(a), 4(a), and 5(a), respectively, except that these charts are for wings with the moment-arm ratio ϵ equal to unity (corresponding to subsonic conditions with the elastic axis fairly far forward on the wing).

The charts of figures 3(c), 4(c), and 5(c) pertain to wings with the moment arm e_1 equal to zero (corresponding roughly to supersonic flow conditions). These figures show the dynamic-pressure parameter ϵq^* defined by either equation (7) or

$$\epsilon q^* = \frac{(1+\lambda)^2}{18432}\frac{C_{L_{\alpha_e}} e_2 \cos\Lambda}{\frac{G}{F_B}\frac{nW}{S}\frac{h_r}{c_r}F_r\eta_a} q \tag{17}$$

plotted against the sweep parameter k/ϵ defined by equation (10) or

$$\frac{k}{\epsilon} = \frac{1+\lambda}{2}\frac{G}{E}\eta_b\frac{A_\Lambda}{\eta_{19}e_2}\tan\Lambda \tag{18}$$

for two values of the stiffness parameter

$$\frac{d}{(k/\epsilon)^2} = \frac{(EI)_r}{(GJ)_r}\left(\frac{e_2 c_r}{s_t}\right)^2 \tag{19}$$

or

$$\frac{d}{(k/\epsilon)^2} = \frac{32}{(1+\lambda)^2}\frac{E}{G}\left(\frac{\eta_{19} e_2}{A_\Lambda}\right)^2 \frac{\eta_6 \eta_7^2}{\eta_8 \eta_9 \eta_{15} \eta_b^2} \tag{20}$$

The various lines of the charts of figures 3 to 5 designate the conditions at which a wing designed on the basis of strength considerations alone is likely to encounter changes in aileron rolling moment by various amounts due to wing flexibility. Those lines for zero rolling moment also designate the conditions at aileron reversal. These charts should be used in conjunction with the preliminary survey charts in reference 2. After it has been found, through the use of the charts in reference 2, to what extent the wing design is affected by such aeroelastic phenomena as divergence and aerodynamic-center shift, the same procedure can be used with the preliminary survey charts in this paper to ascertain whether the wing design is likely to be affected by lateral-control difficulties. If these charts indicate the likelihood of significant aeroelastic effects on the aileron rolling moment, further calculations are desirable. The charts and approximate formulas of this paper may be used for the preliminary calculations; once the structure has been designed, more refined methods, such as that of reference 1, may be used.

Calculation of the Aeroelastic Phenomena Related to Lateral Control

Analysis of the many solutions for the aeroelastic phenomena considered in this paper obtained by the methods given in the appendix shows that the data can be summarized by means of approximate formulas. These formulas involve the aerodynamic, geometric, and structural parameters of the wing through the dimensionless parameters k, k/ϵ, ϵ, and d (equations (9), (10), (11), and (12), respectively) and through a series of constants K_1 to K_7. The constants are functions of the taper ratio, stiffness distribution, and aileron span and are given in table I. As in reference 2, the form of these approximate formulas has been guided by considerations based on an idealized semi-rigid wing, and the actual values of the constants K_3 to K_7 (K_1 and K_2 have been given in reference 2) were obtained by fitting the solution for the functions B_1 to B_6 defined in the appendix by equations (A18) and (A27) to their approximate expressions, equations (A32).

Dynamic pressure at aileron reversal.- The solutions for the aileron reversal speed obtained by the methods given in the appendix can be summarized by approximate formulas which give the dimensionless parameters q^*_R, $(\epsilon q^*)_R$, or $\bar{q}_R$ - that is, the values of the parameters defined in equations (6), (7), and (8) which correspond to the value of the dynamic pressure at aileron reversal - in terms of the parameters k, k/ϵ, ϵ, and d defined by equations (9), (10), (11), and (12), respectively.

An approximate formula for q^*_R is

$$q^*_R = \frac{K_1\left(1 - K_3 \frac{\epsilon}{k} d\right)}{1 + (K_4 + K_2K_3d)\epsilon + K_5d + K_6 \frac{\epsilon}{k} d + K_7k} \tag{21}$$

For very small values of the section moment arm e_1 and the resulting large values of the parameters ϵ and k, the following alternative forms of equation (21) are more convenient to use:

$$(\epsilon q^*)_R = \frac{K_1\left(1 - K_3 \frac{\epsilon}{k} d\right)}{\frac{1}{\epsilon} + K_4 + K_2K_3d + K_5 \frac{1}{\epsilon} d + K_6 \frac{1}{\epsilon} \frac{\epsilon}{k} d + K_7 \frac{k}{\epsilon}} \tag{22}$$

and

$$\bar{q}_R = \frac{K_1\left(1 - K_3 \frac{\epsilon}{k} d\right)}{\frac{1}{k} + \left(K_4 + K_2K_3d\right)\frac{\epsilon}{k} + K_5 \frac{d}{k} + K_6 \frac{\epsilon}{k} \frac{d}{k} + K_7} \tag{23}$$

When the angle of sweep is zero, equations (21) and (22) reduce, respectively, to

$$q^*_R = \frac{K_1}{1 + K_4\epsilon} \tag{24}$$

and

$$(\epsilon q^*)_R = \frac{K_1}{K_4 + \frac{1}{\epsilon}} \tag{25}$$

and when the moment arm e_1 is zero, as it may be in supersonic flow, equations (22) and (23) reduce to

$$(\epsilon q^*)_R = \frac{K_1\left(1 - K_3 \frac{\epsilon}{k} d\right)}{K_4 + K_2K_3d + K_7 \frac{k}{\epsilon}} \tag{26}$$

and

$$\overline{q}_R = \frac{K_1\left(1 - K_3 \frac{\epsilon}{k} d\right)}{K_4 + K_2K_3d \frac{\epsilon}{k} + K_7} \tag{27}$$

The constants K_1 to K_7 are given in table I for wings having half-span outboard ailerons and taper ratios of 0.2, 0.5, and 1.0, for the two different types of stiffness distributions. These constants were found from the results of the numerical matrix method derived in the appendix. Also given in table I are these constants for uniform wings having full-span ailerons and tip ailerons calculated from the results of the analytic integration method of the appendix. Since values of the constants K_1 to K_7 are given for three aileron spans in the case of the uniform wing, they may be interpolated to yield values for other aileron spans. No calculations were made for other than half-span ailerons on tapered wings; nevertheless, as pointed out previously, q_R calculated for half-span ailerons should be reasonably valid for outboard ailerons having spans which differ considerably from one-half.

No aileron-reversal calculations have been made for swept wings with inboard ailerons. However, for unswept uniform wings the dynamic pressure at aileron reversal has been calculated for the limiting case of a wing with an inboard aileron of vanishingly small span by operational methods similar to those described in the appendix in connection with

the calculations for uniform wings. The value of q^*_R obtained in this manner is shown as a function of ϵ in figure 6. Also shown in figure 6 are the values of q^*_R for full-span and for tip ailerons. For small values of ϵ, such as are likely to be encountered in subsonic flight, there is little difference in the values of q^*_R for the three aileron configurations, but at large values of ϵ, such as are likely to be encountered at high-supersonic speeds, there is some difference between them; the aileron reversal speed is highest for the tip aileron and lowest for the inboard aileron. However, these conclusions may not be valid for nonuniform or sweptback wings.

With the values of q^*_R, $(\epsilon q^*)_R$, and $\bar{q}_R$ given by equations (21), (22), and (23) and the definitions of these parameters given by equations (6), (7), and (8), the values of q at aileron reversal may be determined. If desired, the corresponding airspeed may be determined from the relation

$$V_R = \sqrt{\frac{q_R}{\rho/2}} \tag{28}$$

If both q_D (as obtained from reference 2, for instance) and q_R are positive and q_R is greater than q_D, there is no actual aileron reversal speed; in fact, the aileron rolling moment will tend to increase with dynamic pressure until divergence is reached.

The value of q_R calculated for any given value of q^*_R, $(\epsilon q^*)_R$, or $\bar{q}_R$ depends on the value of the effective lift-curve slope $C_{L_{\alpha_e}}$ and, hence, on the Mach number. As suggested in reference 1, the value of q_R may be plotted against Mach number on log-log coordinates; if the straight lines of the actual dynamic pressure at several altitudes as functions of Mach number are drawn on the same plot, an intersection of the reversal line with one of the lines of actual dynamic pressure designates possible aileron reversal at that value of dynamic pressure, Mach number, and altitude.

Spanwise angle-of-attack distribution.- In the appendix, an approximate expression is determined for the change in angle of attack due to the deflection of ailerons on flexible wings. The ratio of the angle-of-attack distribution due to structural deformation α_s to the effective angle of attack of an aileron $\alpha_\delta\delta$ is

$$\frac{\alpha_s}{\alpha_\delta \delta} = \frac{q/q_D}{1 - \frac{q}{q_D}} \frac{(K_4 \epsilon + K_2 k) f_a - K_2 k \, \Delta f_a}{1 - K_2 k} \tag{29}$$

The functions f_a and Δf_a, which depend on the spanwise coordinate s^*, are given in figure 7 for wings having half-span outboard ailerons, taper ratios of 0.2, 0.5, and 1.0, and the two different types of stiffness distribution. The value of q_D required in equation (29) may be found from the approximate expression for q^*_D or $\bar{q}_D$ given in reference 2 as

$$q^*_D = \frac{K_1}{1 - K_2 k} \tag{30}$$

or

$$\bar{q}_D = - \frac{K_1}{K_2 - \frac{1}{k}} \tag{31}$$

When q_D is very large, a more convenient form of equation (29) is as follows:

$$\frac{\alpha_s}{\alpha_\delta \delta} = \frac{\epsilon q^*}{1 - \frac{q}{q_D}} \frac{\left(K_4 + K_2 \frac{k}{\epsilon}\right) f_a - K_2 \frac{k}{\epsilon} \Delta f_a}{K_1} \tag{32}$$

Spanwise lift distribution.- Within the limitations of the modified strip theory used in the analysis, the lift per inch of span is proportional to the local effective angle of attack, so that

$$\frac{l}{\alpha_\delta \delta} = q c C_{l_{\alpha_e}} \left(\frac{\alpha_s}{\alpha_\delta \delta} + 1_a \right) \tag{33}$$

where $\alpha_s/\alpha_\delta \delta$ is obtained as indicated in the preceding section and 1_a is a unit step function of the distance along the span defined by

$1_a = 0$ (when $s < s_i$)

$1_a = 1$ (when $s > s_i$)

The expressions for angle-of-attack deformations and lift distributions (equations (29) and (33)) can be used only for half-span outboard ailerons or spoilers since the functions f_a and Δf_a have been calculated only for this case.

Rolling-moment coefficient and rate of roll due to aileron deflection.- The rolling-moment coefficient due to a unit aileron deflection C_{l_δ} may be obtained in terms of its equivalent rigid-wing value from the approximate formula

$$\frac{C_{l_\delta}}{C_{l_{\delta_0}}} = \frac{1 - \frac{q}{q_R}}{1 - \frac{q}{q_D}} \tag{34}$$

and the wing-tip helix angle due to an aileron deflection pb/2V, which is a measure of the rate of roll and the rolling maneuverability, may be obtained from

$$\frac{pb}{2V} = \left(\frac{pb}{2V}\right)_0 \left(1 - \frac{q}{q_R}\right) \tag{35}$$

The manner in which the aileron-effectiveness parameter $C_{l_\delta}/C_{l_{\delta_0}}$ varies with dynamic pressure depends on the ratio of the reversal to the divergence dynamic pressure as may be seen from equation (34) and figure 8. When the aerodynamic center is ahead of the elastic axis, as is generally the case at subsonic speeds, q_R/q_D is positive and greater than one for sweptforward wings, positive and less than one for unswept wings, and negative for sweptback wings. Thus, in general, $C_{l_\delta}/C_{l_{\delta_0}}$ increases with dynamic pressure until divergence is reached for sweptforward wings; it decreases slowly at first and then more rapidly as reversal is approached for unswept wings; and it decreases rapidly at first and then more slowly for sweptback wings. The rapid decrease in rolling effectiveness for sweptback wings can be alleviated by the use of unconventional lateral-control devices which have their centers of pressure ahead of the elastic axis, such as leading-edge ailerons or spoilers. These devices may also serve to make the dynamic pressure at aileron reversal negative, so that there is no reversal of lateral control in the given speed range. The loss or gain of lateral control is then given by the part of figure 8 for negative values of q/q_R.

The analysis summarized by the approximate formulas (34) and (35) is based on rolling moments about the wing root instead of about the fuselage center line, partly to simplify the analysis and partly to avoid the introduction of the fuselage width as another independent parameter. However, these approximate formulas should be valid for obtaining rolling moments and rates of roll about the fuselage center line as well, because equations (34) and (35) are expressed as ratios of flexible-wing to rigid-wing values; that is, the ratio of the rolling moment about the fuselage center line to its rigid-wing value should be nearly the same as the ratio of the equivalent rolling moment about the wing root to its rigid-wing value when the ratio of the fuselage width to the wing span is small.

The rolling-moment coefficient and rates of roll given by equations (34) and (35) are functions of the aileron span inasmuch as q_R is a function of the aileron span. The variation of C_{l_δ} or $pb/2V$ with aileron span can therefore be found only for uniform wings; however, since the effect of aileron span on q_R is not very great, its effect on C_{l_δ} or $pb/2V$ is not likely to be great. In the case of uniform wings, the rolling moment due to the deflection of an inboard aileron can be found by superposition because the aeroelastic equations upon which the results of this paper are based are linear; that is, the rolling-moment coefficient due to a 30-percent-span inboard aileron, for example, is equal to C_{l_δ} for a full-span aileron minus C_{l_δ} for a 70-percent-span outboard aileron.

Inertia effects.- In steady rolling flight no inertia effects are present which can affect the static aeroelastic problem except, possibly, for centrifugal forces on heavy underslung nacelles. The maximum value of $pb/2V$ is therefore usually unaffected by inertia effects. However, in the equally important problem of initial rolling acceleration, which governs the time in which a given rolling velocity can be attained, inertia effects must usually be taken into account. In reference 2 the observation was made that in symmetric flight inertia effects are not as important as other static aeroelastic effects, except for flying wings, because the inertia forces are in about the same ratio to the aerodynamic forces as the wing weight is to the airplane weight. By the same reasoning, inertia effects are almost always very important in getting into a roll because the inertia forces are then in about the same ratio to the aerodynamic forces as the moment of inertia of the wings about the longitudinal axis of the airplane is to the moment of inertia of the entire airplane about its longitudinal axis, a ratio which is usually close to 1.

No charts are presented in this paper for these inertia effects because the manner in which mass is distributed varies so widely among

different airplanes that preparation of a generally applicable set of charts appears to be impractical at present. However, the procedure outlined in reference 2 for taking inertia effects into account in the calculation of quasi-static aeroelastic phenomena by means of the charts presented therein may be applied to the calculation of the inertia effects encountered in starting a roll. This procedure is described in the following paragraphs.

For a given rolling acceleration $\dot{p}$, the linear normal acceleration of an element of mass at a distance y from the center line of the airplane is $\dot{p}y$. From this linear acceleration and the known or estimated mass distribution of the wing, the inertia load l_i per inch of span and the inertia torque t_i per inch of span can be calculated for any given normal, pitching, or rolling acceleration. Substitution of these loads and torques for the terms l and le_1c in equations (A3) or (A36) and equations (A2) or (A35) of reference 2, respectively, yields the values of the accumulated bending moments and torques in equations (A4) and (A5) or in equations (A37) and (A38) of reference 2. Equation (A6) of reference 2, or the matrix equivalent of this equation, then yields the angle-of-attack distribution due to the deformations caused by the inertia effects associated with the given acceleration.

This angle-of-attack distribution can be considered as a geometrical angle-of-attack distribution. For the purpose of calculating the increment caused by aeroelastic action, this distribution can be approximated by a linear-twist angle-of-attack distribution with a value at the wing tip which is such that the moment about the effective wing root of the area under the linear-twist distribution equals the moment of the area under the calculated angle-of-attack distribution due to inertia effects. (The moment, rather than the area, is suggested as a basis of correlation because the angles of attack near the wing tip are more important in aeroelastic phenomena than those at the wing root.) The justification for this rather arbitrary approximation to the angle-of-attack distribution is that the correction to be applied as a result of aeroelastic action to the deformations due to inertia loads is usually small compared with these deformations.

The angle of attack due to structural deformation α_s associated with the linear-twist distribution can then be obtained from equation (21) and figure 7 of reference 2 or, if $\lambda = 0$, from figure 8 of reference 2. The lift distribution associated with the total angle-of-attack distribution due to the deformations caused by the inertia effects, including the increment in this angle-of-attack distribution produced by aeroelastic action, can then be found from equation (24b) of reference 2, in which α_g, α_{g_t}, and l_0 pertain to the calculated angle-of-attack distribution due to the inertia effects (not the linear approximation to

this distribution). This lift distribution can be integrated to obtain the rolling moment due to inertia effects, as modified by aeroelastic action.

The rolling moment calculated in this manner may then be combined with the rolling moment due to aileron or spoiler deflection, which may be calculated as indicated in the preceding section. If the contributions of the tail and the fuselage to the rolling moment are neglected,

$$\dot{p}(\bar{I} - \bar{I}_w) = \frac{1}{144} C_{l_{\delta_s}} \delta qSb + \left(\frac{\partial L'_w}{\partial \dot{p}}\right)_s \dot{p}$$

where $\dot{p}$ is the angular acceleration in roll, $\bar{I}$ is the mass moment of inertia of the entire airplane about its longitudinal axis, $\bar{I}_w$ is the mass moment of inertia of both wings about the longitudinal axis of the airplane, and $C_{l_{\delta_s}}$ is the flexible-wing value of the rolling-moment coefficient due to aileron deflection (which may be calculated in the manner described in the preceding section). The ratio $(\partial L'_w/\partial \dot{p})_s$ is the rolling moment per unit rolling acceleration due to inertia effects, including aeroelastic effects, and is equal to $-I_w$ plus the rolling moment due to the lift which results from the deformations due to the inertia loads per unit angular acceleration in roll as well as from the aeroelastic deformations which accompany these inertia deformations; in other words, $(\partial L'_w/\partial \dot{p})_s$ is equal to $-\bar{I}_w$ plus the rolling moment calculated as described in the preceding paragraphs for $\dot{p} = 1$. Then

$$\dot{p} = \frac{1}{144} \frac{1}{1 - \frac{1}{\bar{I} - \bar{I}_w}\left(\frac{\partial L'_w}{\partial \dot{p}}\right)_s} \frac{C_{l_{\delta_s}} \delta qSb}{\bar{I} - \bar{I}_w} \tag{36a}$$

or

$$\dot{p} = \frac{1}{144} \frac{C_{l_{\delta_{s,i}}} \delta qSb}{\bar{I} - \bar{I}_w} \tag{36b}$$

where

$$C_{l_{\delta_s,i}} \equiv \frac{1}{1 - \frac{1}{\bar{I} - \bar{I}_w}\left(\frac{\partial L'_w}{\partial \dot{p}}\right)_s} C_{l_{\delta_s}}$$

is a rolling-moment coefficient per unit aileron deflection which includes static aeroelastic effects, inertia effects, and the aeroelastic magnification of the inertia effects. This rolling-moment coefficient is a truer index of the rate at which a roll can be initiated than $C_{l_{\delta_s}}$. The initial rolling acceleration (disregarding unsteady-lift effects) can be calculated from equations (36).

Illustrative Example

The approximate formulas described in the preceding sections have been used to find the effects of aeroelasticity on some lateral-control properties of the wing considered in the illustrative example of reference 2. The resulting calculations are an extension of those in reference 2, and the additional parameters are presented in table II.

The subsonic and supersonic values of the parameters k, ϵ, and d were calculated from equations (9), (11), and (12), respectively. With the appropriate values of the factors K_1 to K_7 interpolated from table I, the values of q^*_R were calculated from equation (21) and are given in table II. From these values of q^*_R, the subsonic and supersonic dynamic pressures at aileron reversal were found by means of equation (6). These values of q_R vary as the reciprocal of the effective lift-curve slope, if the corresponding values of e_1 and e_2 are assumed to remain constant.

In order to find the angle-of-attack distributions due to deflections of the aileron from equation (29), the values of the functions f_a and Δf_a were taken from figure 7(c). The spanwise change in angle of attack is shown in the top plot of figure 9 for different values of the dynamic-pressure ratio. The rolling-moment coefficient and wing-tip helix angle due to deflections of the aileron were calculated from equations (34) and (35) and were plotted in figure 9 as functions of the dynamic-pressure ratio $\frac{q}{-q_D}$.

DISCUSSION

Limitations of the Charts and Approximate Formulas

The charts and the approximate formulas presented in this paper are subject to certain limitations as a result of the approximations made in the calculations on which they are based. These limitations are discussed fully in reference 2 and can be classified as restrictions on the plan form, on the speed regime, and on the wing structure. The limitations are given very briefly as follows:

(1) The results obtainable by the use of the charts and approximate formulas are likely to be unsatisfactory for wings of very low aspect ratio, very large sweep, or zero taper ratio

(2) The results are restricted to wings on which the spanwise lift distribution is roughly proportional to the chord and angle of attack and on which the section aerodynamic centers are at an approximately constant fraction of the chord; these restrictions are most likely to be violated by wings flying at transonic speeds and by wings having concentrated sources of lift, such as nacelles and tip tanks

(3) The results are somewhat restricted to wings with one of the two types of spanwise stiffness distributions used in the analysis, wings with no chordwise bending (relatively thick wings), and wings having an elastic axis at an approximately constant fraction of the chord.

The manner in which the aeroelastic effects of aileron deflection are analyzed in the present paper imposes certain additional limitations that particularly affect the aileron geometry. In the analysis in the appendix, the spanwise lift distribution due to the deflection of an aileron was approximated by strip theory, an approximation which is probably less valid for aileron deflections than for geometric angles of attack. The assumption was also made that the centers of pressure due to aileron deflections are at a constant fraction of the wing chord; this assumption is also probably less valid than the assumption that the section aerodynamic centers of the wing are at a constant fraction of the chord. Since these assumptions are more nearly true for wings of high than those of low aspect ratio, these limitations serve, in effect, to restrict the applicability of the present paper to aspect ratios somewhat higher than those amenable to the analyses of reference 2.

The results of the present paper do not take into account explicitly any flexibility of the aileron itself because of the assumption that the angle between the aileron and wing is constant along the span of the

aileron. This assumption is almost universally made in analyzing the aeroelastic properties of ailerons and is justifiable because the net effect of the difference between the wing deformations and the aileron deformations on the over-all lift and moments appears to be negligible.

As a result of the fact that the static aeroelastic phenomena associated with lateral control involve many more parameters than do those associated with symmetric flight, the coverage of the various parameters is not as complete as in reference 2. Specifically, angle-of-attack distributions have been presented only for uniform wings, all the charts and approximate formulas presented in this paper are restricted to outboard lateral-control devices (ailerons or spoilers) except for the uniform-wing case, and most of the calculations upon which these results are based were made for wings with half-span outboard ailerons ($s^*_1 = 0.5$). However, the results of the analysis for the uniform wings with full-span ailerons ($s^*_1 = 0$) and tip ailerons ($s^*_1 \rightarrow 1$) indicate that, except for the angle-of-attack distributions, the results based on a half-span aileron are approximately valid for outboard ailerons of spans differing considerably from one-half.

Relation between Strength and Stiffness as Design Criteria

The relation between strength and stiffness as design criteria was discussed in reference 2. The preliminary survey charts in reference 2 indicate the extent to which a wing designed on the basis of strength considerations alone is likely to be affected by aeroelastic phenomena and, consequently, indicate whether the wing has to be stiffened beyond the amount associated with the required strength. The preliminary survey charts of this paper (figs. 3 to 5) serve the same purpose in regard to the aeroelastic effects on lateral control; furthermore, even though the charts of reference 2 may indicate that a particular wing is not significantly affected by the aeroelastic phenomena considered in that paper, this wing may still have to be stiffened because of an undesirably large loss in lateral control.

As may be concluded from the survey charts of reference 2 and the present paper, as well as from the discussion contained in reference 2, the following wings designed on the basis of strength considerations are most likely to be subject to adverse aeroelastic effects on lateral control and rolling maneuverability:

(1) Wings with a high design flying speed or dynamic pressure

(2) Sweptback wings

(3) Thin wings

(4) Wings designed for low wing loading

(5) Unswept and moderately swept wings with an elastic axis relatively far forward on the chord or with the center of pressure of the lift produced by aileron deflections relatively far back on the chord as a result of the aileron configuration (small aileron chord or wing of low aspect ratio) or flight condition (supersonic speeds)

(6) Wings with a relatively high lift-curve slope

Structural Weight Associated with the Required Stiffness

When a given wing has been shown to be subject to undesirably large aeroelastic effects by means of the charts of reference 2 and the present paper or by any other method, the problem arises how to distribute the additional required stiffness; that is, which spanwise distribution of structural material will alleviate the adverse aeroelastic phenomena to the desired extent with the minimum increase in structural weight.

In order to shed some light on this problem, aeroelastic and weight calculations have been made for a family of somewhat arbitrarily selected stiffness distributions which differ from the distribution required by the constant-stress criterion in a manner described in reference 2. These stiffness distributions are designated by the tip-stiffness-ratio parameter ω, which is the ratio of the stiffness EI or GJ at the wing tip to the corresponding stiffness of a constant-stress wing. The results of the lateral-control calculations for wings with taper ratio 0.5, with constant wing-thickness ratio h/c along the span, and with two of these stiffness distributions are included in table I and figure 7(b). The designation "excess strength" refers to the stiffness distribution increased over the constant-stress requirement to such an extent that the value of ω is 2.0. The results of the aeroelastic calculations for the stiffness distributions decreased below the constant-stress requirement to a value of $\omega = 0.5$ happen to be the same as the results for the constant-stress stiffness distributions for wings with varying wing-thickness ratio; that is, $\frac{(h/c)_t}{(h/c)_r} = 0.5$. The structural weight considered in these calculations is that of the primary load-carrying structure; the remaining structure is assumed to be unchanged in the stiffening process.

The results of the weight calculations and aeroelastic calculations in reference 2 indicated that the addition of stiffness in the outboard regions of a wing (large values of ω) was more efficient, from weight considerations, in alleviating the aeroelastic effects considered in that paper than the addition of stiffness in the inboard regions. This conclusion is corroborated, in essence, by the calculations made for the aeroelastic phenomena considered in the present paper. Figure 10, which consists of a plot of the structural weights required for a given loss in lateral control at a constant value of dynamic pressure, indicates that the least weight is associated with values of the tip-stiffness-ratio parameter ω greater than 1, except for wings with values of the sweep parameters k or k/ϵ equal to -8. These large negative values of k or k/ϵ, however, pertain to wings that are (1) sweptforward, (2) sweptback with the aerodynamic center behind the elastic axis (in the case of negative k), or (3) sweptback with the center of pressure due to aileron deflection ahead of the elastic axis (in the case of negative k/ϵ, as it may be for spoilers or leading-edge ailerons). For sweptforward wings, the aileron rolling moment usually increases rather than decreases with dynamic pressure; lateral control then does not impose any structural requirements so that the curves do not have much significance for such wings.

The Aeroisoclinic Wing

It was shown in reference 2 that an over-all type of aeroisoclinicism in which bending and torsion action tend to cancel for the wing as a whole can be achieved for the aeroelastic phenomena considered in that paper by a choice of a suitable ratio of the bending to the torsion stiffness or by a choice of the elastic-axis location, that is, by satisfying the relation

$$\frac{s_t}{e_1 c_r} \frac{(GJ)_r}{(EI)_r} \tan \Lambda = \frac{1}{K_2} \tag{37}$$

(where K_2 is given in table I). However, reference 2 indicates that even if the conditions of equation (37) are achieved, there may still be great losses in lateral control and the wing may still be subject to adverse dynamic phenomena; in fact, the severity of adverse aeroelastic effects in the lateral control and of certain dynamic phenomena may be increased as a result of achieving aeroisoclinicism.

The results of the present paper corroborate the conclusion concerning aeroelastic effects on lateral control. However, by suitable

additional modifications a wing which has been made aeroisoclinic can also be made to suffer no loss in lateral control due to aeroelastic action. As may be seen from figures 3 to 5 or from equation (34), the condition for no losses in lateral control is that q_R be equal to q_D; or, by setting equation (21) equal to equation (30), that

$$K_4\epsilon + (K_2 + K_7)k + K_5 d + (K_3 + K_6)\frac{\epsilon}{k} d = 0 \tag{38}$$

of which the condition

$$\frac{s_t}{e_2 c_r} \frac{(GJ)_r}{(EI)_r} \tan \Lambda = - \frac{1}{K_2} \tag{39}$$

usually is an approximate solution. Therefore, in order to satisfy both of the conditions specified in equations (37) and (38), the section moment arm e_2 must be nearly equal to $-e_1$ or, in other words, the center-of-pressure parameters a and cp_δ must be nearly equal, a condition which can be satisfied by using full-chord ailerons (all-movable wing tips), or a combination of geared leading- and trailing-edge ailerons, for instance. However, as pointed out in reference 2, attempts at solving static aeroelastic problems by aiming at aeroisoclinicism may tend to aggravate certain dynamic phenomena. The same statement must also be made concerning the foregoing methods of alleviating static aeroelastic effects on lateral control; these methods may, for instance, lead to flutter difficulties which may require excessive mass balancing of the control surfaces.

Relation of Charts to Design Procedure

The conventional procedure of designing a wing on the basis of strength requirements and later checking it for aeroelastic effects can be facilitated at several stages by using the methods described in the present paper and in reference 2. As pointed out in reference 2, for instance, the preliminary-survey charts presented therein can be used to establish some static aeroelastic characteristics that would be obtained in symmetric flight if the wing were designed for strength alone.

If these characteristics are deemed satisfactory, the design can proceed on the basis of strength requirements alone. If, on the other hand, they are considered unsatisfactory, the wing must be stiffened.

The amount of additional material required can be estimated, as indicated in reference 2, by interpolating between the results presented therein for the constant-strength case, the "excess strength" case, and the case $\frac{(h/c)_t}{(h/c)_r} = 0.5$. As previously mentioned, the additional structural material is usually most effective if distributed near the wing tip.

Similarly, the preliminary-survey charts of the present paper can be used to ascertain whether the wing can meet lateral-control requirements if designed for strength alone. If it must be stiffened to meet these requirements, the necessary amount of additional material can be estimated in the same manner as indicated in reference 2 for aeroelastic effects incurred in symmetric flight.

Inasmuch as the charts of reference 2 and of the present paper pertain only to static aeroelastic phenomena, the problem remains of ascertaining in the preliminary design stage whether a wing designed for strength alone (or, for that matter, a wing designed both on the basis of strength requirements and of static aeroelastic considerations) is likely to experience flutter difficulties. However, flutter is a much more complicated phenomenon and depends on many more parameters than do static aeroelastic phenomena. Consequently, preparation of a generally applicable set of charts appears impractical. Nonetheless, although phenomenologically or functionally flutter is not related to the static aeroelastic phenomena considered in reference 2 and the present paper, it is "mechanically" related by virtue of the fact that all these phenomena depend on the wing geometry and the wing stiffness (although the aerodynamic parameters are different and flutter, unlike the static aeroelastic phenomena, involves the mass distribution of the wing and the damping properties of the structure). On the basis of past experience, certain qualitative conclusions can be drawn concerning this relation.

As shown in the charts of this paper, the aileron reversal speed, or the speed at which a specified amount of control is retained, is lower for highly sweptback wings than for unswept wings. Similarly, the divergence speed decreases rapidly as the angle of sweepforward increases. For a typical wing the values of q^* at divergence and at reversal as obtained by the charts of this paper are shown as a function of the sweep parameter k in figure 11. For unswept wings the dynamic pressure at flutter is usually within a certain range varying between a value lower than the dynamic pressure at reversal to a value higher than the dynamic pressure at divergence, depending on the geometric, structural, aerodynamic, and mass parameters of the given case, and varying even for a given case and a given speed range with altitude, because a change in air density may change the mode in which

the wing flutters. This wide range is indicated in figure 11 by starting three flutter curves at $k = 0$; these curves do not necessarily constitute the upper and lower limits.

If the variation of flutter speed with sweep angle is assumed for the purpose of illustration to be similar to that indicated in figure 17 of reference 7, the three flutter curves of figure 11 are obtained. This figure must not be construed as presenting any quantitative information; to emphasize this point the wing is not identified. Even qualitatively the relation between the dynamic pressures at flutter, divergence, and reversal is subject to certain limitations because the flutter tests of reference 7 were performed

(1) At subsonic speeds

(2) On models without ailerons

(3) On models without concentrated masses

(4) With models which fluttered in the classical two-degree-of-freedom mode

There is reason to believe that sweptback wings with high aspect ratios flying at high altitudes may experience a possibly mild form of flutter in a single-degree-of-freedom mode, because a vertical motion necessarily implies vertical bending and, hence, in the case of a swept wing, a variation in the angle of attack. In general, the greater the number of degrees of freedom the more difficult it is to relate flutter to the static aeroelastic phenomena.

However, at subsonic speeds and low or moderately high altitudes at least, the trend shown in figure 11 should be valid for wings without very large concentrated masses and with irreversible controls, which tend to minimize the possibility of aileron-coupled flutter. Consequently, if these wings are highly swept back they can be designed to meet lateral-control requirements with the likelihood that they will then be safe against flutter as well, provided conventional lateral-control devices are used. On the other hand, if these wings are unswept or even moderately swept back, they may have to be stiffened beyond the amount required by static aeroelastic considerations.

In any event the final design must be checked both for static aeroelastic effects and for flutter. In most cases the static aeroelastic effects can probably be calculated with sufficient accuracy by means of the charts and approximate formulas of reference 2 and the present paper. In some cases, however, particularly if these effects are in any way critical, a more refined method of analysis, such as that of references 1 and 8, may have to be used.

CONCLUDING REMARKS

An approximate method based on charts and approximate formulas has been presented for estimating rapidly the aeroelastic effects on the lateral control of swept and unswept wings at subsonic and supersonic speeds. The charts and approximate formulas presented in this paper together with those presented in NACA TN 2608 also serve to simplify design procedure in many instances because they can be used at the preliminary design stage to estimate the amount of additional material required to stiffen a wing which is strong enough and because they indicate that the best way of distributing this additional material is to locate most of it near the wing tip in most cases.

For the purpose of making specific calculations, the limitations of the method of this paper are that they do not apply directly to wings with very low aspect ratio, with very large angles of sweep, with zero taper ratio, or with large sources of concentrated aerodynamic forces.

The charts and approximate formulas indicate that the control effectiveness of an airplane may be increased by varying some of the design parameters such as the ratio of torsional to bending stiffness and, if necessary, resorting to unconventional lateral-control devices. The charts also indicate that a wing which is strong enough is most likely to be affected by losses in lateral control due to wing flexibility if it is to operate at high dynamic pressures, if it is thin, if it has a large angle of sweepback, if it has an elastic-axis location relatively far forward on the chord or a location of the center of pressure due to aileron deflection far rearward on the chord, or if it is to operate at transonic or high-supersonic Mach numbers.

Langley Aeronautical Laboratory
National Advisory Committee for Aeronautics
Langley Field, Va., March 7, 1952

APPENDIX

METHODS OF CALCULATIONS ON WHICH CHARTS ARE BASED

The Aeroelastic Equations

The assumptions made in the following analysis are the same as those made in reference 2:

(1) Aerodynamic induction is taken into account by applying an over-all correction to strip theory

(2) Aerodynamic and elastic forces are based upon the assumption of small deflections

(3) The wing is clamped at the root perpendicular to a straight elastic axis, and all deformations are considered to be given by the elementary theories of bending and torsion about the elastic axis

In addition it is assumed, as in reference 1 and elsewhere, that the angle between the aileron and the wing is constant along the span of the aileron. Then, for a wing with an outboard aileron, the force per unit width on sections perpendicular to the elastic axis is

$$l = \frac{qcC_{L_{\alpha_e}}}{144}\left(\alpha_s + \alpha_\delta \delta 1_a\right) \tag{A1}$$

where 1_a is a unit step function of s defined by

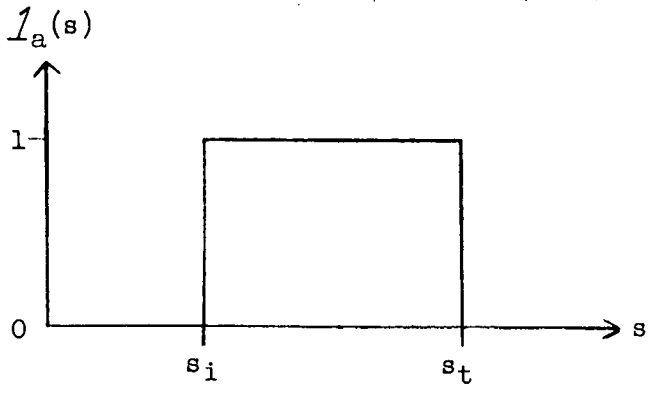

where s_i is the spanwise ordinate of the inboard end of the aileron. The running torque of this force about the elastic axis is

$$\frac{qc^2e_1C_{L_{\alpha_e}}}{144}\left(\alpha_s - \epsilon\alpha_\delta\delta\mathit{l}_a\right) \tag{A2}$$

where ϵ is the moment-arm ratio e_2/e_1.

The integration of these forces yields the accumulated torque and bending moment:

$$T = \frac{qc_r^2e_1C_{l_{\alpha_e}}}{144}\int_s^{s_t}\left(\frac{c}{c_r}\right)^2\left(\alpha_s - \epsilon\alpha_\delta\delta\mathit{l}_a\right)ds \tag{A3}$$

$$M = \frac{qc_rC_{L_{\alpha_e}}}{144}\int_s^{s_t}\int_s^{s_t}\frac{c}{c_r}\left(\alpha_s + \alpha_\delta\delta\mathit{l}_a\right)ds\,ds \tag{A4}$$

Combining these equations with the equations of elastic deformation presented in appendix A of reference 2 as

$$\varphi = \int_0^s \frac{1}{GJ}T\,ds$$

$$\Gamma = \int_0^s \frac{1}{EI}M\,ds$$

results in two simultaneous equations of equilibrium:

$$\frac{d}{ds}\left(GJ\,\frac{d\varphi}{ds}\right) = -\frac{qc^2e_1C_{L_{\alpha_e}}}{144}\left[(\varphi\cos\Lambda - \Gamma\sin\Lambda) - \epsilon\alpha_\delta\delta\underline{]}_a\right] \tag{A5}$$

$$\frac{d^2}{ds^2}\left(EI\,\frac{d\Gamma}{ds}\right) = \frac{qcC_{L_{\alpha_e}}}{144}\left[(\varphi\cos\Lambda - \Gamma\sin\Lambda) + \alpha_\delta\delta\underline{]}_a\right] \tag{A6}$$

These equations are subject to the following boundary conditions:

$$\varphi(0) = 0 \tag{A7a}$$

$$\Gamma(0) = 0 \tag{A7b}$$

$$\left(GJ\,\frac{d\varphi}{ds}\right)_{s=s_t} = 0 \tag{A7c}$$

$$\left(EI\,\frac{d\Gamma}{ds}\right)_{s=s_t} = 0 \tag{A7d}$$

$$\left(EI\,\frac{d^2\Gamma}{ds^2}\right)_{s=s_t} = 0 \tag{A7e}$$

The angle of attack due to structural deformations is related to φ and Γ by the equation

$$\alpha_s = \varphi\cos\Lambda - \Gamma\sin\Lambda \tag{A8}$$

After equations (A5) and (A6) have been solved, the rolling moment about the wing root may be found from the expression

$$\frac{qS\,\frac{b}{2}\,C_l}{144} = T_r \sin\Lambda + M_r \cos\Lambda \tag{A9}$$

where the root twisting moment T_r and the root bending moment M_r are given by equations (A3) and (A4) evaluated at s equal to zero. Then the rolling-moment ratio becomes

$$\frac{C_{l_\delta}}{C_{l_{\delta_0}}} = 1 + \frac{\frac{d}{k}(B_1 + \epsilon B_2) + B_3 + \epsilon B_4}{\frac{d}{k}\epsilon B_5 + B_6} \tag{A10}$$

where the functions B_1 to B_6 are defined by

$$B_1 + \epsilon B_2 = \int_0^1 \left(\frac{c}{c_r}\right)^2 \frac{\alpha_s}{\alpha_\delta \delta}\, ds^* \tag{A11a}$$

$$B_3 + \epsilon B_4 = \int_0^1 \int_0^{s^*} \frac{c}{c_r} \frac{\alpha_s}{\alpha_\delta \delta}\, ds^*\, ds^* \tag{A11b}$$

$$B_5 = -\int_0^1 \left(\frac{c}{c_r}\right)^2 \mathcal{I}_a\, ds^* \tag{A11c}$$

$$B_6 = \int_0^1 \int_0^{s^*} \frac{c}{c_r} \mathcal{I}_a\, ds^*\, ds^* \tag{A11d}$$

and where the parameter d/k is defined by

$$\frac{d}{k} = \frac{e_1 c_r}{s_t} \tan \Lambda \tag{A12}$$

Solution for Uniform Wings

If the torsional stiffness, the bending stiffness, and the chord of the wing have constant values of $(GJ)_r$, $(EI)_r$, and c_r, respectively, along the wing span, the equations of equilibrium (A5) and (A6) become

$$\varphi'' \cos \Lambda = -q^* \left[(\varphi \cos \Lambda - \Gamma \sin \Lambda) - \epsilon \alpha_\delta \delta \mathcal{I}_a \right] \tag{A13}$$

$$\Gamma''' \sin \Lambda = -\bar{q} \left[(\varphi \cos \Lambda - \Gamma \sin \Lambda) + \alpha_\delta \delta \mathcal{I}_a \right] \tag{A14}$$

where the differentiation denoted by the prime is with respect to $\xi \equiv 1 - \frac{s}{s_t}$.

Differentiating equation (A13) once with respect to ξ and combining it with equation (A14) yields the single differential equation of equilibrium,

$$\alpha_s''' + q^* \alpha_s' - \bar{q} \alpha_s = \alpha_\delta \delta \; q^* \epsilon \mathcal{I}_a' + \bar{q} \mathcal{I}_a \tag{A15}$$

subject to the following boundary conditions:

$$\alpha_s(1) = 0 \tag{A16a}$$

$$\alpha_s'(0) = 0 \tag{A16b}$$

$$\alpha_s''(0) = -q^* \left[\alpha_s(0) - \epsilon \alpha_\delta \delta \mathcal{I}_a(0) \right] \tag{A16c}$$

The complete solution of equation (A15) can be readily obtained by means of Laplace transforms as

$$\frac{\alpha_s(\xi)}{\alpha_\delta \delta} = q^*(1+\epsilon)\left[f_5(\xi) - f_5(\xi - \xi_i) - \frac{f_5(1) - f_5(1-\xi_i)}{f_3(1)} f_3(\xi)\right] + \frac{f_3(1-\xi_i)}{f_3(1)} f_3(\xi) - f_3(\xi - \xi_i) - \mathcal{I}_a(\xi) \tag{A17}$$

where the functions $f_3(\xi)$ and $f_5(\xi)$, as well as $f_4(\xi)$ which will be used subsequently, are defined in appendix A of reference 2 as

$$f_3(\xi) = C_1 e^{-2\beta\xi} + e^{\beta\xi}\left(C_2 \cos \gamma\xi + \frac{C_3}{\gamma} \sin \gamma\xi\right)$$

$$f_4(\xi) = C_4 e^{-2\beta\xi} + e^{\beta\xi}\left(C_5 \cos \gamma\xi + \frac{C_6}{\gamma} \sin \gamma\xi\right)$$

$$f_5(\xi) = C_7 e^{-2\beta\xi} + e^{\beta\xi}\left(C_8 \cos \gamma\xi + \frac{C_9}{\gamma} \sin \gamma\xi\right)$$

where the constants of integration are defined in reference 2 in terms of the roots of the characteristic equation, -2β and $\beta \pm i\gamma$. These three functions are equal to zero when $\xi < 0$.

The substitution of this solution into equations (A11) yields the functions

$$B_1(q^*,k) = \frac{f_3(1-\xi_i)}{f_3(1)} f_4(1) - f_4(1-\xi_i) - \xi_i + B_2 \tag{A18a}$$

$$B_2(q^*,k) = \frac{1}{k}\left[f_3(1) - f_3(1-\xi_i)\right] + q^*\left[\frac{1}{k} - \frac{f_4(1)}{f_3(1)}\right]\left[f_5(1) - f_5(1-\xi_i)\right] \tag{A18b}$$

$$B_3(q^*,k) = \frac{f_3(1 - \xi_i)}{f_3(1)} f_5(1) - f_5(1 - \xi_i) - \xi_i + \frac{1}{2}\xi_i^2 + B_4 \qquad (A18c)$$

$$B_4(q^*,k) = \frac{1}{k^2}\left[f_3(1) - f_3(1 - \xi_i)\right] + \frac{1}{k}\left[f_4(1) - f_4(1 - \xi_i)\right] +$$

$$q^*\left[\frac{1}{k^2} - \frac{f_5(1)}{f_3(1)}\right]\left[f_5(1) - f_5(1 - \xi_i)\right] - \frac{1}{k}\xi_i \qquad (A18d)$$

$$B_5 = -\xi_i \qquad (A18e)$$

$$B_6 = \xi_i - \frac{1}{2}\xi_i^2 \qquad (A18f)$$

The value of q^* at reversal is that value which makes $C_{l_\delta}/C_{l_{\delta_0}}$ in equation (A10) equal to zero for given values of the parameters k, ϵ, and d.

For a full-span aileron ($\xi_i = 1$), equations (A18) become

$$B_1(q^*,k) = \frac{f_4(1)}{f_3(1)} - 1 + B_2 \qquad (A19a)$$

$$B_2(q^*,k) = \frac{1}{k}\left[f_3(1) - 1\right] + q^*\left[\frac{1}{k} - \frac{f_4(1)}{f_3(1)}\right]f_5(1) \qquad (A19b)$$

$$B_3(q^*,k) = \frac{f_5(1)}{f_3(1)} - \frac{1}{2} + B_4 \qquad (A19c)$$

$$B_4(q^*,k) = \frac{1}{k^2}\left[f_3(1) - 1\right] + \frac{1}{k}\left[f_4(1) - 1\right] + q^*\left[\frac{1}{k^2} - \frac{f_5(1)}{f_3(1)}\right]f_5(1) \quad \text{(A19d)}$$

$$B_5 = -1 \quad \text{(A19e)}$$

$$B_6 = \frac{1}{2} \quad \text{(A19f)}$$

and for a "tip aileron" of very short span ($\xi_i \to 0$), equations (18) become

$$B_1(q^*,k) = \xi_i\left\{f_3(1) + q^*\left[f_4(1) - kf_5(1)\right]\frac{f_4(1)}{f_3(1)} - 1\right\} + B_2 \quad \text{(A20a)}$$

$$B_2(q^*,k) = \xi_i\left[q^*f_5(1) - q^*\frac{f_4(1)}{f_3(1)}f_4(1)\right] \quad \text{(A20b)}$$

$$B_3(q^*,k) = \xi_i\left\{f_4(1) + q^*\left[f_4(1) - kf_5(1)\right]\frac{f_5(1)}{f_3(1)} - 1\right\} + B_4 \quad \text{(A20c)}$$

$$B_4(q^*,k) = \xi_i\left\{\frac{1}{k}\left[f_3(1) - 1\right] + q^*\left[\frac{1}{k} - \frac{f_4(1)}{f_3(1)}\right]f_5(1)\right\} \quad \text{(A20d)}$$

$$B_5 = -\xi_i \quad \text{(A20e)}$$

$$B_6 = \xi_i \quad \text{(A20f)}$$

Solution for Nonuniform Wings

By means of strip theory applied at a finite number of points, equation (A1) may be written in matrix notation as

$$\{l\} = \frac{qC_{L_{\alpha_e}}}{144} \lfloor c \rfloor \left\{ \{\alpha_s\} + \alpha_\delta \delta \{\mathcal{I}_a\} \right\} \tag{A21}$$

and the expression for torque (A2) as

$$\frac{qe_1 C_{L_{\alpha_e}}}{144} \lfloor c^2 \rfloor \left\{ \{\alpha_s\} - \epsilon\alpha_\delta \delta \{\mathcal{I}_a\} \right\} \tag{A22}$$

The matrix notation used in this analysis is the same as in reference 1.

Equations (A3) and (A4), written in matrix notation, are

$$\{T\} = \frac{qc_r^2 e_1 s_t}{144} C_{L_{\alpha_e}} [I'] \left\lfloor \left(\frac{c}{c_r}\right)^2 \right\rfloor \left\{ \{\alpha_s\} - \epsilon\alpha_\delta \delta \{\mathcal{I}_a\} \right\} \tag{A23}$$

$$\{M\} = \frac{qc_r s_t^2}{144} C_{L_{\alpha_e}} [II'] \left\lfloor \frac{c}{c_r} \right\rfloor \left\{ \{\alpha_s\} + \alpha_\delta \delta \{\mathcal{I}_a\} \right\} \tag{A24}$$

where the integrating matrices $[I']$ and $[II']$ are, respectively, for single and double integration from tip to root and are given in reference 1. The value of $\{\mathcal{I}_a\}$ at the matrix station nearest the discontinuity of $\mathcal{I}_a$ can be modified as in reference 1 in such a manner that premultiplication of $\{\mathcal{I}_a\}$ by $\lfloor I'_1 \rfloor$ and $\lfloor II'_1 \rfloor$ yields the same area and moment about the wing root, respectively, as would be obtained by analytic integration. This modification may also be regarded as an attempt to round off the lift distribution near the inboard end of the aileron in a physically reasonable manner.

The combination of equations (A23) and (A24) with matrix expressions for $\{\varphi\}$ and $\{\Gamma\}$ in terms of $\{T\}$ and $\{M\}$ (see appendix A of reference 2) yields the matrix equilibrium equation,

$$\left[[1] - q^*[A]\right]\{\alpha_s\} = -q^*\alpha_\delta\delta\{\beta\} \tag{A25}$$

which can be solved for $\{\alpha_s\}$. The aeroelastic matrix $[A]$ is defined in reference 1 and the column matrix $\{\beta\}$ is defined by

$$\{\beta\} = \left[\epsilon[I]''\left[\frac{(GJ)_r}{GJ}\right][I']\left[\left(\frac{c}{c_r}\right)^2\right] + k[I]''\left[\frac{(EI)_r}{EI}\right][II']\left[\frac{c}{c_r}\right]\right]\{1_a\} \tag{A26}$$

After the rolling-moment ratio expressed by equation (A10) is set equal to zero, the condition for aileron reversal is

$$\frac{d}{k}(B_1 + \epsilon B_2) + B_3 + \epsilon B_4 + \frac{d}{k}\epsilon B_5 + B_6 = 0$$

where the matrix equivalents of equations (A11) become

$$B_1 + \epsilon B_2 = \frac{1}{\alpha_\delta\delta}[I'1]\left[\left(\frac{c}{c_r}\right)^2\right]\{\alpha_s\} \tag{A27a}$$

$$B_3 + \epsilon B_4 = \frac{1}{\alpha_\delta\delta}[II'1]\left[\frac{c}{c_r}\right]\{\alpha_s\} \tag{A27b}$$

$$B_5 = -[I'1]\left[\left(\frac{c}{c_r}\right)^2\right]\{1_a\} \tag{A27c}$$

$$B_6 = [II'1]\left[\frac{c}{c_r}\right]\{1_a\} \tag{A27d}$$

Therefore, the condition for aileron reversal expressed in matrix notation is

$$\left[\frac{d}{k}\left[I'_1\right]\left[\left(\frac{c}{c_r}\right)^2\right] + \left[II'_1\right]\left[\frac{c}{c_r}\right]\right]\{\alpha_s\} = \alpha_\delta\delta\left[\frac{d}{k}\epsilon\left[I'_1\right]\left[\left(\frac{c}{c_r}\right)^2\right] - \left[II'_1\right]\left[\frac{c}{c_r}\right]\right]\{1_a\} \tag{A28}$$

Solving equation (A28) for $\alpha_\delta\delta$ and multiplying the resulting equation by $\{\beta\}$ yields

$$\alpha_\delta\delta\,\{\beta\} = \frac{\{\beta\}\left[\frac{d}{k}\left[I'_1\right]\left[\left(\frac{c}{c_r}\right)^2\right] + \left[II'_1\right]\left[\frac{c}{c_r}\right]\right]\{\alpha_s\}}{\left[\frac{d}{k}\epsilon\left[I'_1\right]\left[\left(\frac{c}{c_r}\right)^2\right] - \left[II'_1\right]\left[\frac{c}{c_r}\right]\right]\{1_a\}} \tag{A29}$$

The substitution of this expression for $\alpha_\delta\delta\,\{\beta\}$ into the equilibrium equation (A25) yields

$$\{\alpha_s\} = q^*_R\left[A_R\right]\{\alpha_s\} \tag{A30}$$

where the aileron-reversal matrix $\left[A_R\right]$ is defined by

$$\left[A_R\right] = \left[A\right] - \frac{1}{\left[\frac{d}{k}\epsilon\left[I'_1\right]\left[\left(\frac{c}{c_r}\right)^2\right] - \left[II'_1\right]\left[\frac{c}{c_r}\right]\right]\{1_a\}}\{\beta\}\left[\frac{d}{k}\left[I'_1\right]\left[\left(\frac{c}{c_r}\right)^2\right] + \left[II'_1\right]\left[\frac{c}{c_r}\right]\right] \tag{A31}$$

The value of q^* at aileron reversal can be found by the iteration of this aileron-reversal matrix.

Representation of Results by Approximate Formulas

Approximate formulas, similar to those in reference 2, have been used to combine the results of the many computations indicated in this analysis; as in the case of the formulas presented in reference 2, those presented in this section are based on considerations of a semi-rigid wing.

The functions B_1 to B_5 in equation (A10) have been found to be given quite accurately by the following approximate expressions:

$$B_1 = -B_6 \frac{q^*/q^*_D}{1 - \frac{q^*}{q^*_D}} \frac{K_5 k}{1 - K_2 k} \tag{A32a}$$

$$B_2 = -B_6 \frac{q^*/q^*_D}{1 - \frac{q^*}{q^*_D}} \frac{K_3 + K_6}{1 - K_2 k} \tag{A32b}$$

$$B_3 = -B_6 \frac{q^*/q^*_D}{1 - \frac{q^*}{q^*_D}} \frac{(K_2 + K_7)k}{1 - K_2 k} \tag{A32c}$$

$$B_4 = -B_6 \frac{q^*/q^*_D}{1 - \frac{q^*}{q^*_D}} \frac{K_4}{1 - K_2 k} \tag{A32d}$$

$$B_5 = -B_6 K_3 \tag{A32e}$$

where the factors K_4 to K_7 depend on the aileron span, the taper ratio, and the spanwise variation of the bending and torsion stiffnesses. The factor K_2 is independent of the aileron span, and the factor K_3 is independent of the stiffness variation.

The following approximate formula may be obtained by the substitution of equations (A32) into equation (A10):

$$\frac{C_{l_\delta}}{C_{l_{\delta_0}}} = \frac{1 - \frac{q}{q_R}}{1 - \frac{q}{q_D}} \tag{A33}$$

where the value of q at aileron reversal is

$$q_R = \frac{q_D(1 - K_2k)\left(1 - K_3 \frac{\epsilon}{k} d\right)}{1 + (K_4 + K_2K_3d)\epsilon + K_5d + K_6 \frac{\epsilon}{k} d + K_7k} \tag{A34}$$

With the use of the approximate formula presented in reference 2,

$$q^*_D = \frac{K_1}{1 - K_2k} \tag{A35}$$

equation (A34) becomes

$$q^*_R = \frac{K_1\left(1 - K_3 \frac{\epsilon}{k} d\right)}{1 + (K_4 + K_2K_3d)\epsilon + K_5d + K_6 \frac{\epsilon}{k} d + K_7k} \tag{A36}$$

The accuracy of equation (A36) compared with the results calculated directly by the method of the preceding section is illustrated in figures 6 and 12.

The results of reference 2 indicate that the damping-in-roll derivative may be expressed approximately by

$$C_{l_p} = C_{l_{p_0}} \frac{1}{1 - \frac{q}{q_D}} \tag{A37}$$

and since the wing-tip helix angle due to roll is

$$\frac{pb}{2V} = -\frac{C_{l_\delta}}{C_{l_p}} \tag{A38}$$

an approximate formula for rolling maneuverability is

$$\frac{pb}{2V} = \left(\frac{pb}{2V}\right)_0 \left(1 - \frac{q}{q_R}\right) \tag{A39}$$

Figure 13 shows the approximate formulas (A33) and (A39) to be in good agreement with more accurately computed values.

An approximate expression for the structural twist due to aileron deflection similar to the expressions for the structural twists due to geometrical angles of attack given in reference 2 has been deduced from the results of the analysis in the preceding section:

$$\frac{\alpha_s}{\alpha_\delta \delta} = \frac{q/q_D}{1 - \frac{q}{q_D}} \frac{(K_4 \epsilon + K_2 k) f_a - K_2 k \, \Delta f_a}{1 - K_2 k} \tag{A40}$$

where f_a and Δf_a are functions of the spanwise coordinate s^*, the wing chord and stiffness variations, and the aileron span. The accuracy of equation (A40) is indicated in figure 14.

REFERENCES

1. Diederich, Franklin W.: Calculation of the Lateral Control of Swept and Unswept Flexible Wings of Arbitrary Stiffness. NACA Rep. 1024, 1951. (Supersedes NACA RM L8H24a.)

2. Diederich, Franklin W., and Foss, Kenneth A.: Charts and Approximate Formulas for the Estimation of Aeroelastic Effects on the Loading of Swept and Unswept Wings. NACA TN 2608, 1952.

3. Malvestuto, Frank S., Jr., and Hoover, Dorothy M.: Lift and Pitching Derivatives of Thin Sweptback Tapered Wings with Streamwise Tips and Subsonic Leading Edges at Supersonic Speeds. NACA TN 2294, 1951.

4. Cohen, Doris: Formulas and Charts for the Supersonic Lift and Drag of Flat Swept-Back Wings with Interacting Leading and Trailing Edges. NACA TN 2093, 1950.

5. Harmon, Sidney M., and Jeffreys, Isabella: Theoretical Lift and Damping in Roll of Thin Wings with Arbitrary Sweep and Taper at Supersonic Speeds. Supersonic Leading and Trailing Edges. NACA TN 2114, 1950.

6. Diederich, Franklin W.: A Plan-Form Parameter for Correlating Certain Aerodynamic Characteristics of Swept Wings. NACA TN 2335, 1951.

7. Barmby, J. G., Cunningham, H. J., and Garrick, I. E.: Study of Effects of Sweep on the Flutter of Cantilever Wings. NACA Rep. 1014, 1951. (Supersedes NACA TN 2121.)

8. Diederich, Franklin W.: Calculation of the Aerodynamic Loading of Swept and Unswept Flexible Wings of Arbitrary Stiffness. NACA Rep. 1000, 1950. (Supersedes NACA TN 1876.)

TABLE I

VALUES OF THE COEFFICIENTS K_1 TO K_7

λ	GJ and EI	$\frac{(h/c)_t}{(h/c)_r}$	s^*_i	K_1	K_2	K_3	K_4	K_5	K_6	K_7
1.0	Vary as c^4	1.0	0	2.47	0.390	2.000	1.028	0.615	-0.285	-0.020
1.0		1.0	.5	2.58	.381	1.362	.972	.715	.194	.028
1.0		1.0	1.0	2.47	.390	1.000	.822	.850	.310	.129
.5		1.0	.5	2.83	.480	.891	1.009	.643	.159	.025
.2		1.0	.5	2.92	.590	.633	1.035	.567	.134	-.016
1.0	Given by constant-stress criterion	1.0	.5	.795	.252	1.362	.946	.430	-.011	-.010
.5		1.0	.5	1.287	.357	.891	.923	.410	-.025	-.031
.2		1.0	.5	1.830	.480	.633	.872	.392	-.047	-.053
.5		.5	.5	.928	.310	.891	.852	.335	-.105	-.051
.5	Increased beyond values required by constant-stress criterion	1.0	.5	1.700	.398	.891	.975	.433	-.006	-.015

TABLE II

PARAMETERS OF EXAMPLE WING

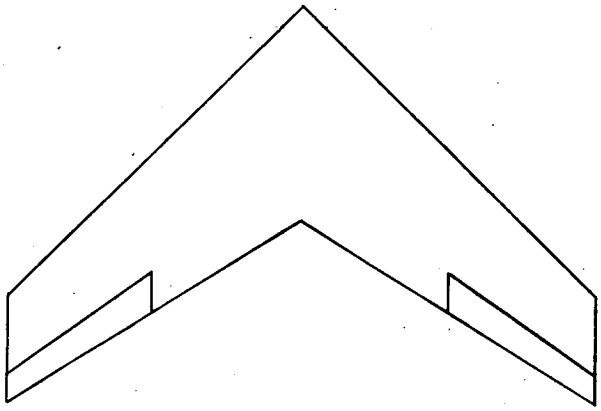

Parameter	Subsonic (M = 0)	Supersonic (M = 1.5)
s^*_i	0.5	0.5
e_2	0.016	0.458
ϵ	0.082	24.1
k	7.76	79.0
d	0.551	0.551
K_1	2.82	2.82
K_2	0.474	0.474
K_3	0.917	0.917
K_4	1.006	1.006
K_5	0.650	0.650
K_6	0.160	0.160
K_7	0.026	0.026
q^*_D	-1.053	-0.0774
q^*_R	1.687	0.0713
q_R, lb/sq ft	10,300	2,500
f_a	See fig. 7(c)	See fig. 7(c)
Δf_a	See fig. 7(c)	See fig. 7(c)
$\alpha_s/\alpha_\delta\delta$	See equation (29)	See equation (29)
$C_{l_\delta}/C_{l_{\delta_0}}$	$\frac{1 + 0.624 \frac{q}{q_D}}{1 - \frac{q}{q_D}}$	$\frac{1 + 1.085 \frac{q}{q_D}}{1 - \frac{q}{q_D}}$
$\frac{(pb/2V)}{(pb/2V)_0}$	$1 + 0.624 \frac{q}{q_D}$	$1 + 1.085 \frac{q}{q_D}$

NACA

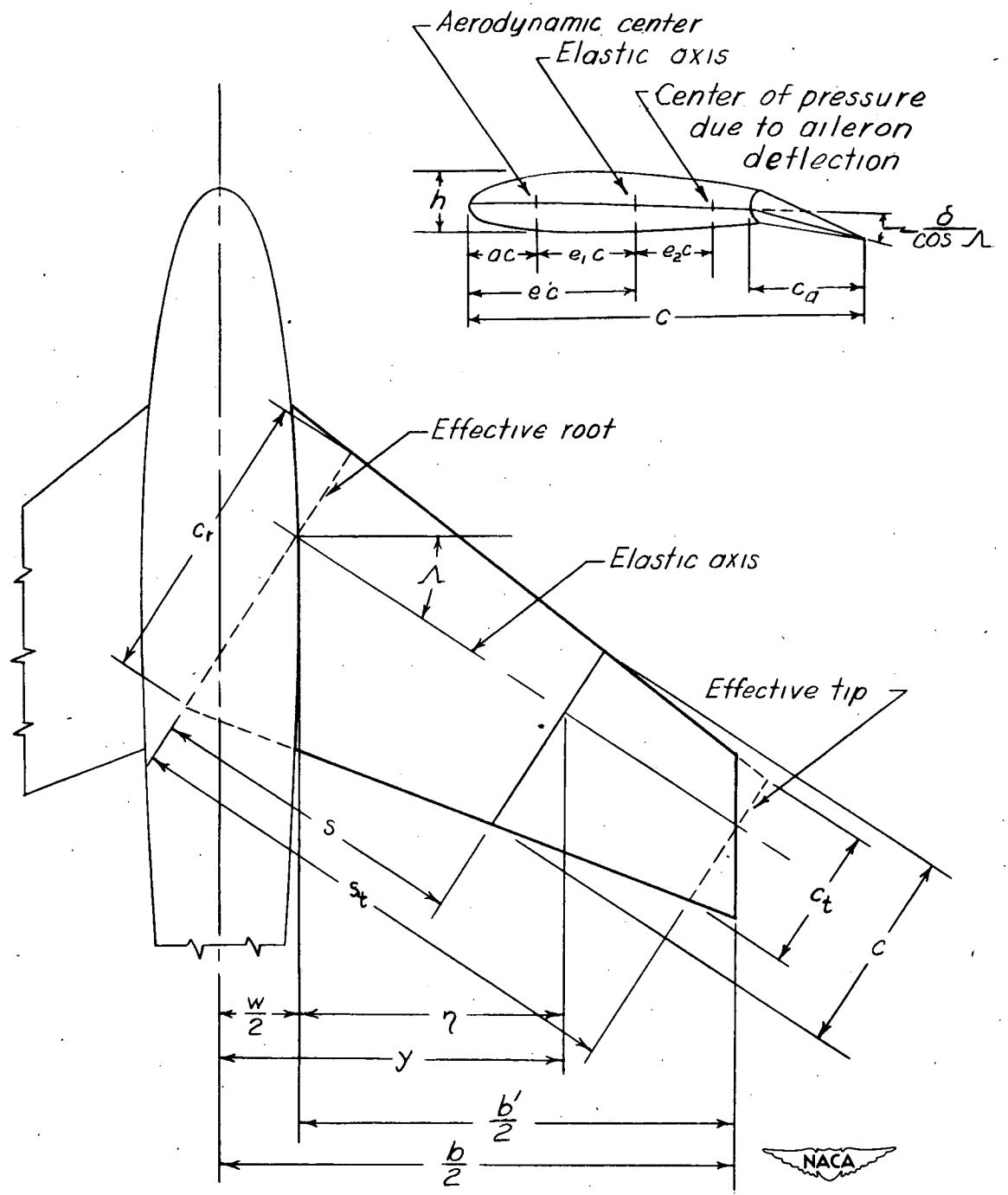

Figure 1.- Definitions of geometric parameters.

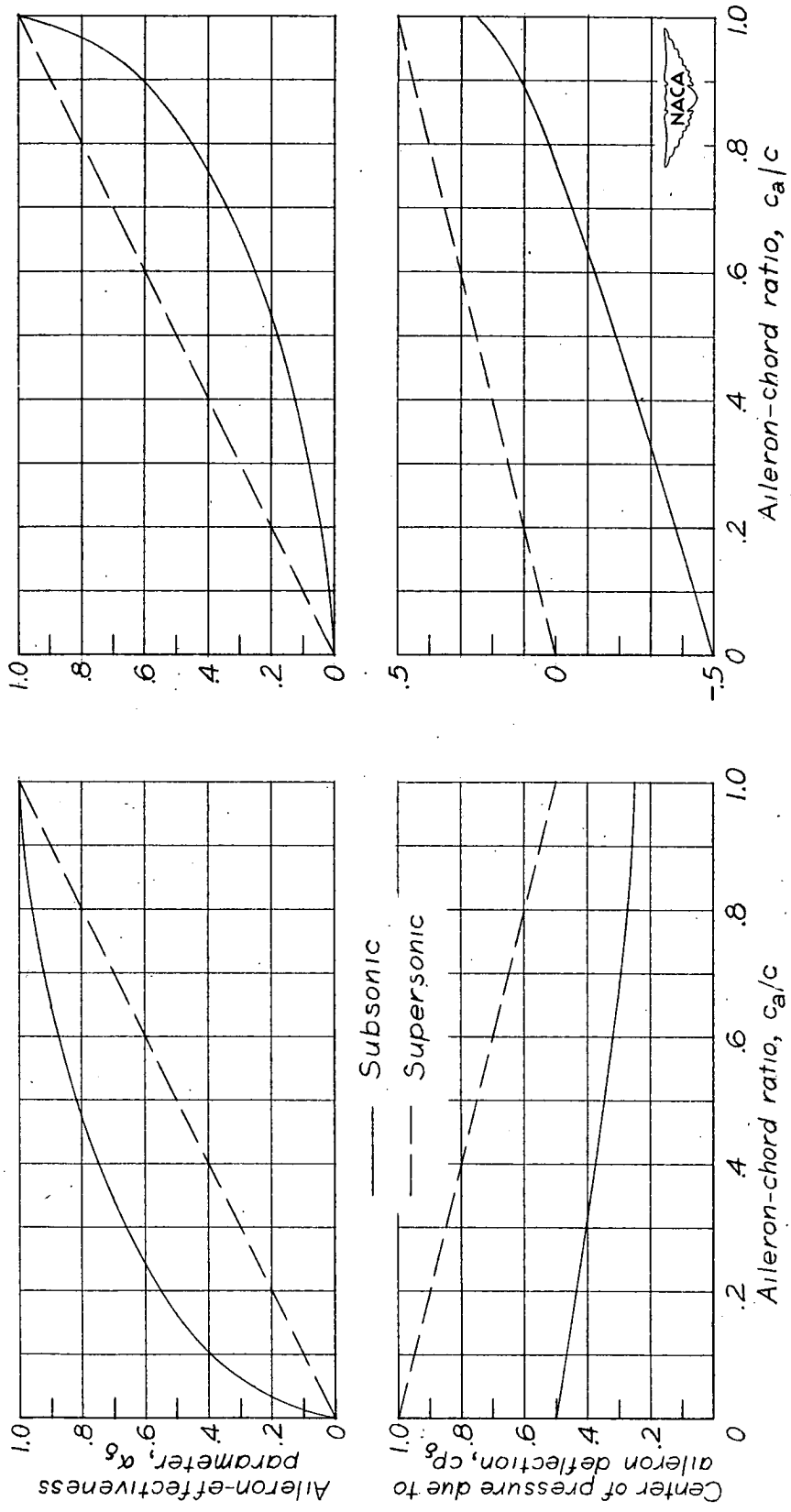

(a) Trailing-edge ailerons. (b) Leading-edge ailerons.

Figure 2.- Theoretical two-dimensional values of the aileron-force parameters.

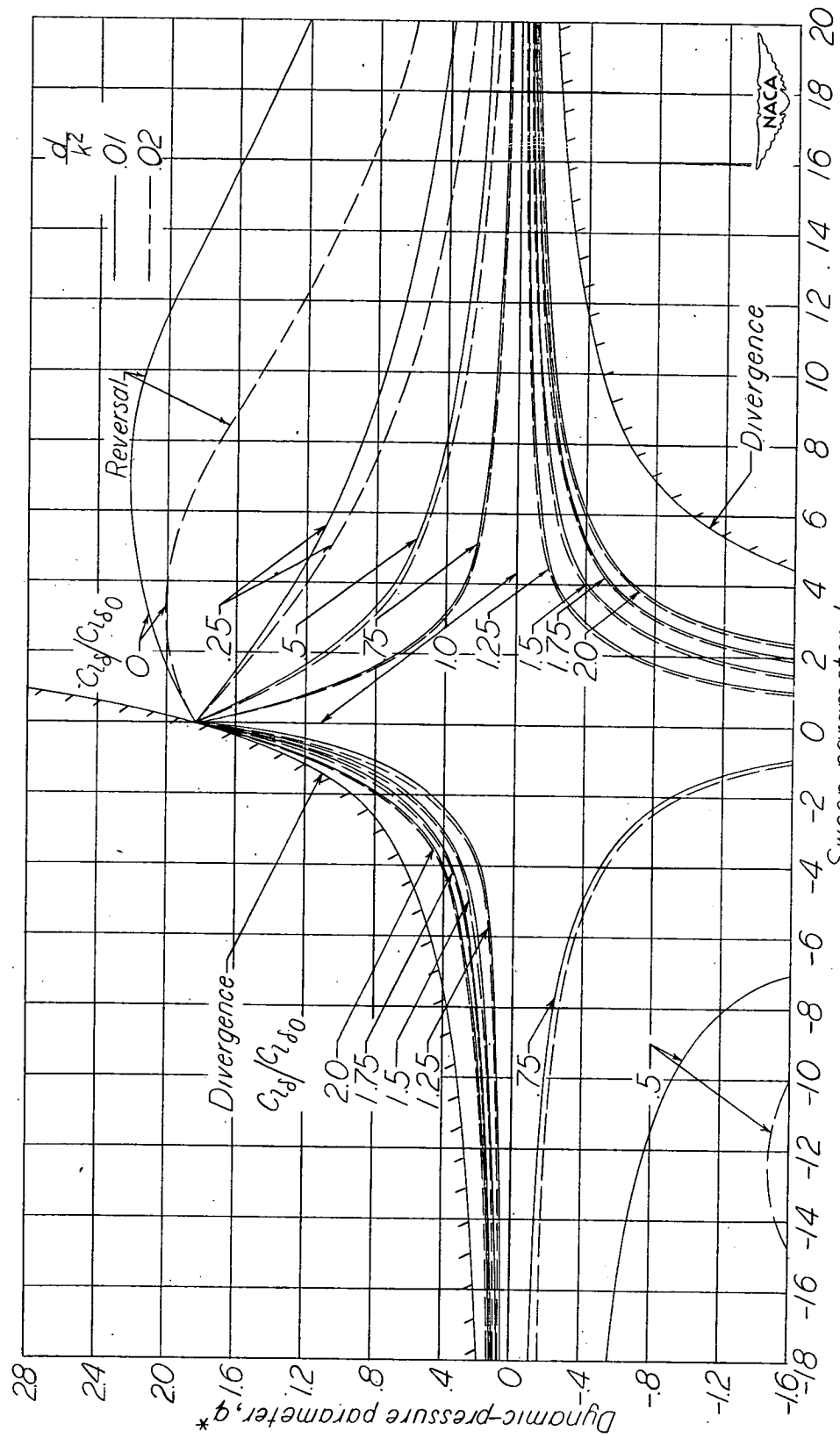

(a) Wings with moment arm $e_2 = 0$.

Figure 3.- Charts for a preliminary survey of lateral control for flexible wings of taper ratio 0.2.

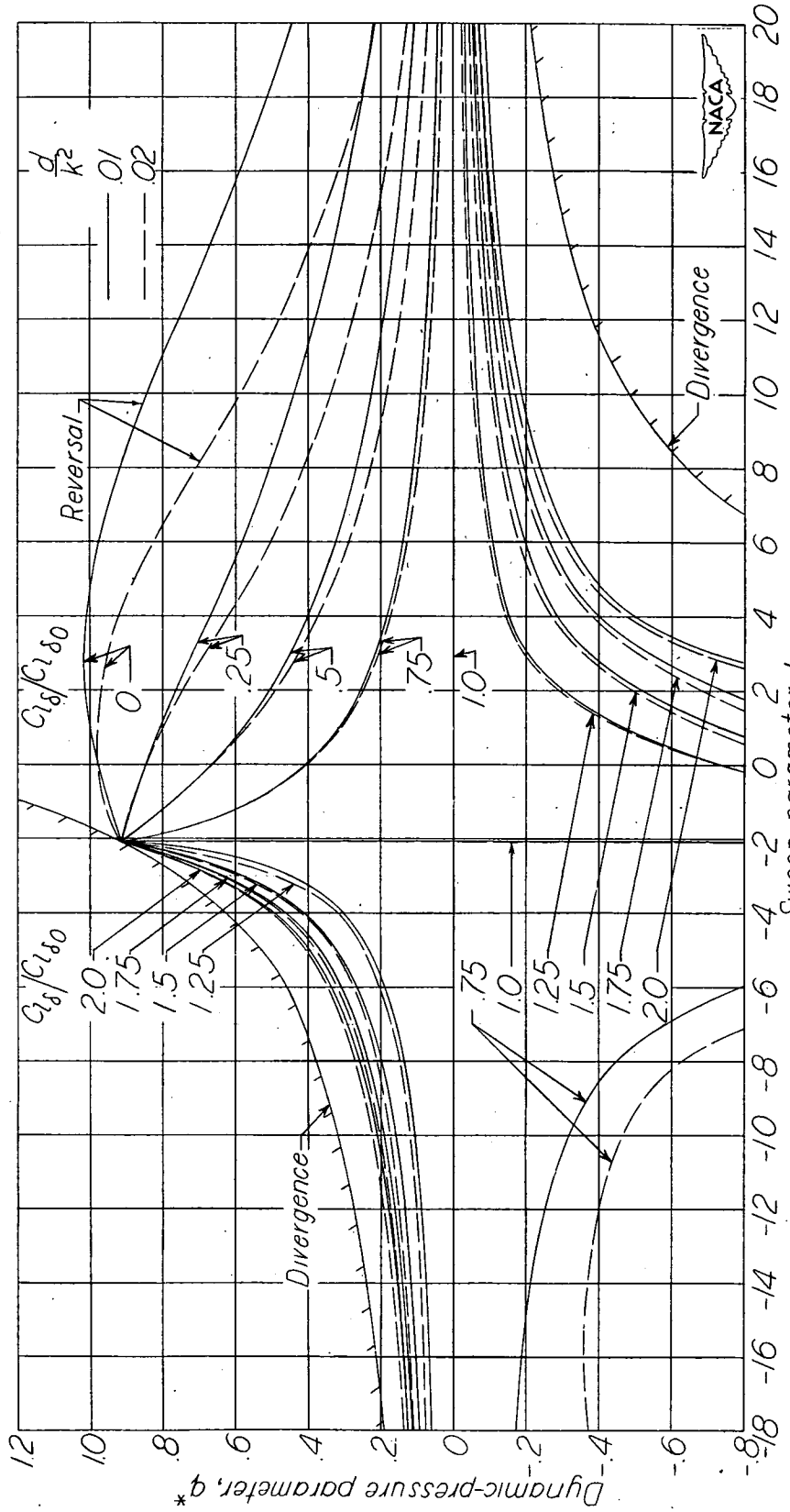

(b) Wings with moment-arm ratio $\epsilon = 1.0$.

Figure 3.- Continued.

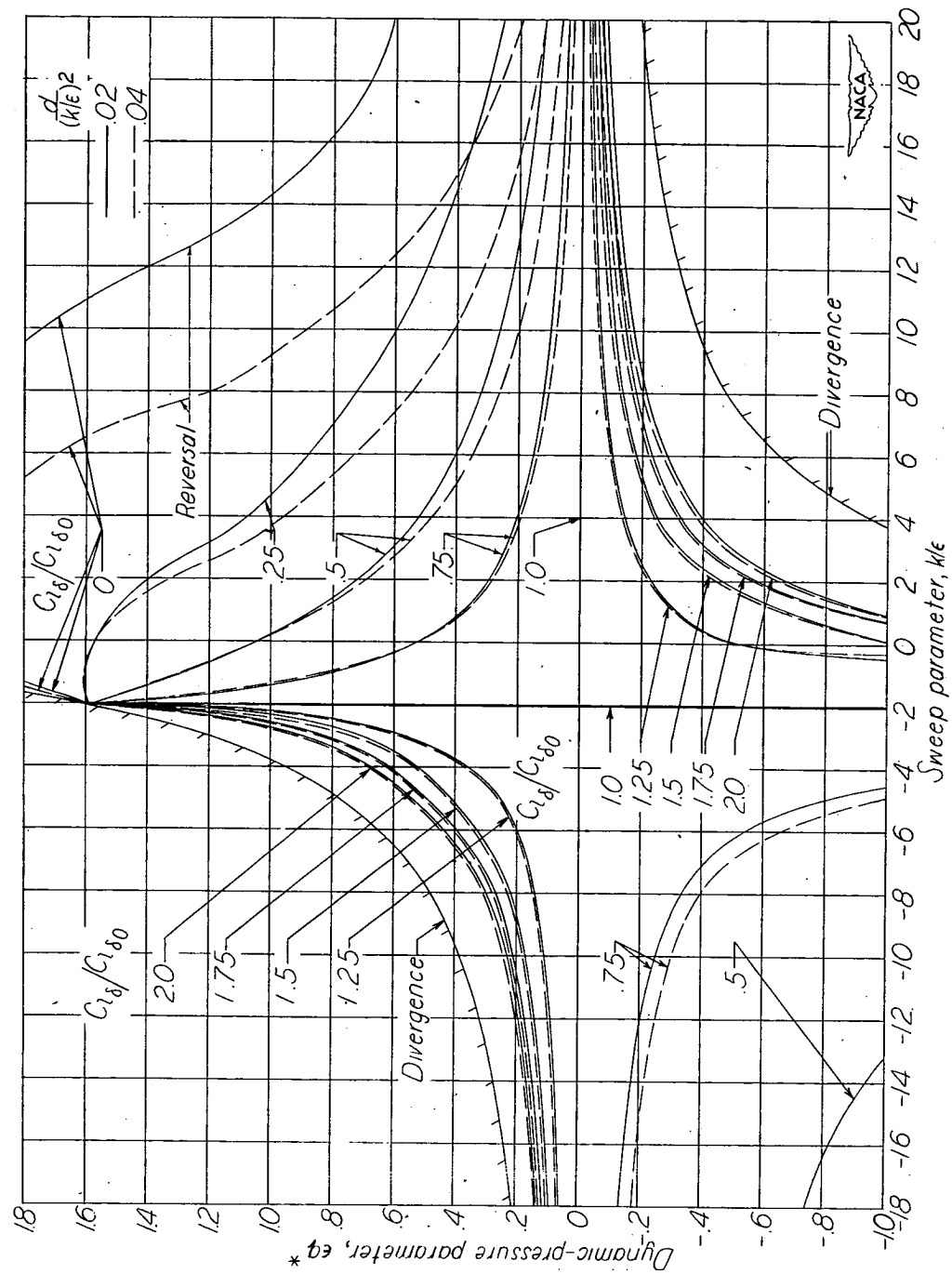

(c) Wings with moment arm $e_1 = 0$.

Figure 3.- Concluded.

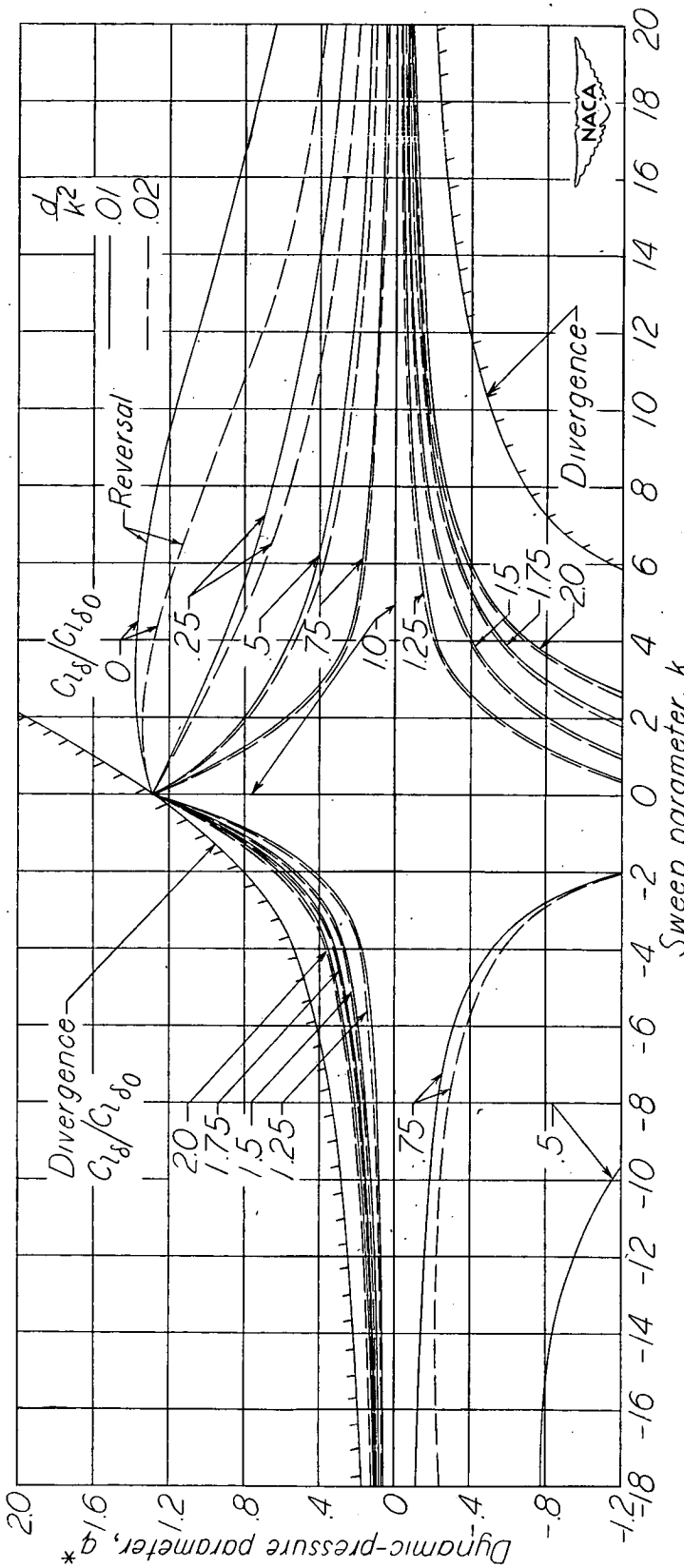

(a) Wings with moment arm $e_2 = 0$.

Figure 4.- Charts for a preliminary survey of lateral control for flexible wings of taper ratio 0.5.

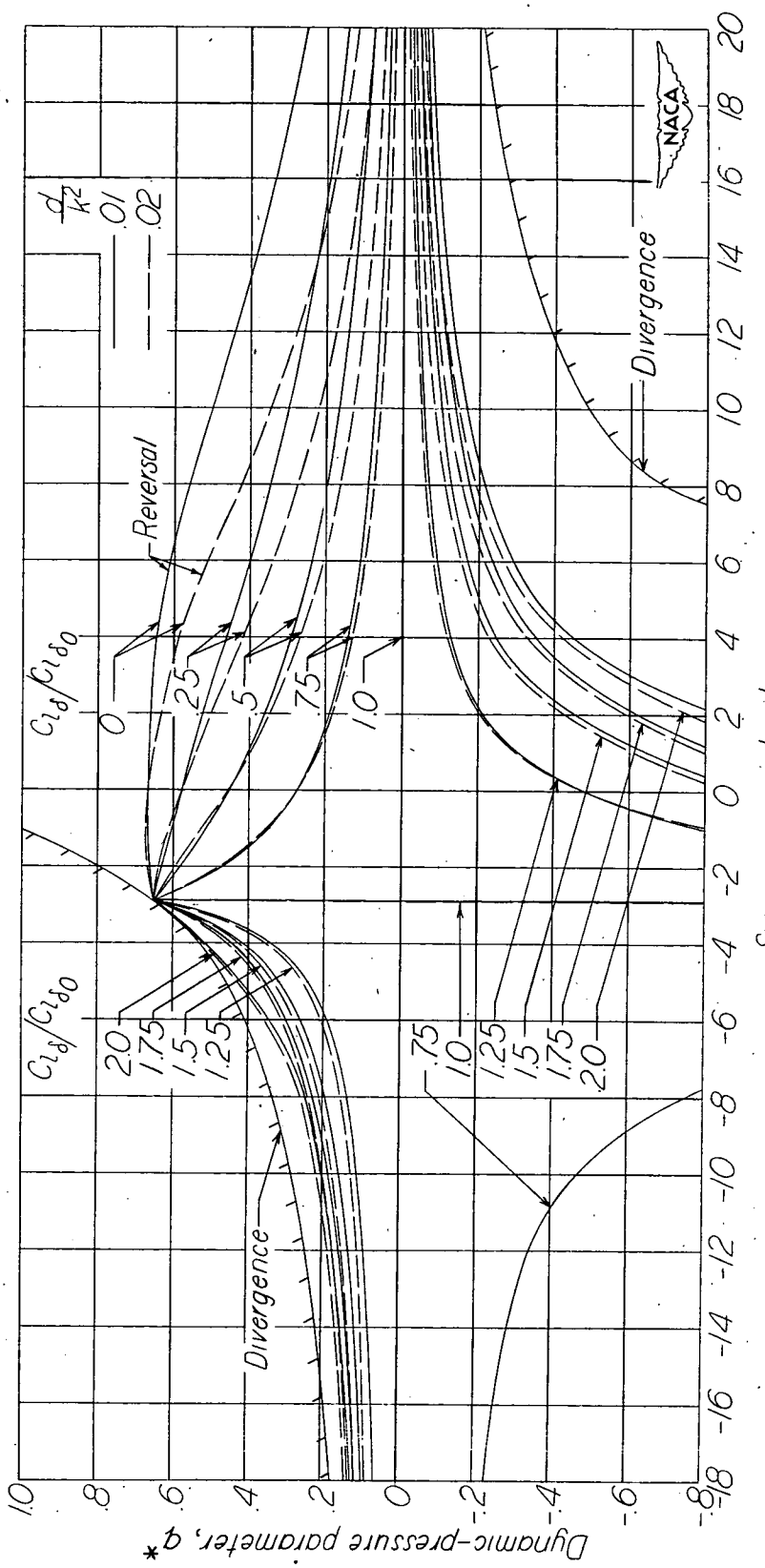

(b) Wings with moment-arm ratio $\epsilon = 1.0$.

Figure 4.- Continued.

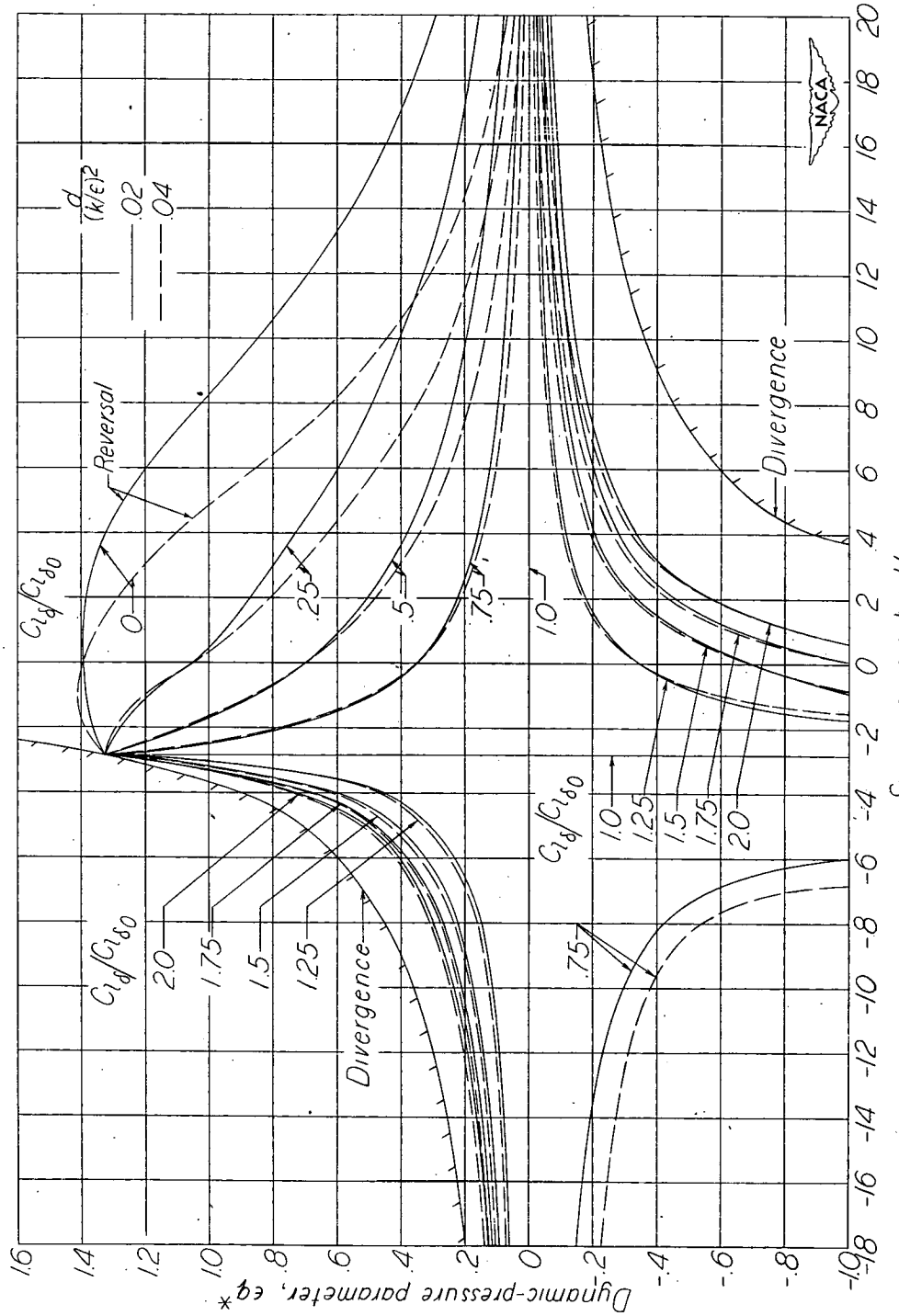

(c) Wings with moment arm $e_1 = 0$.

Figure 4.- Concluded.

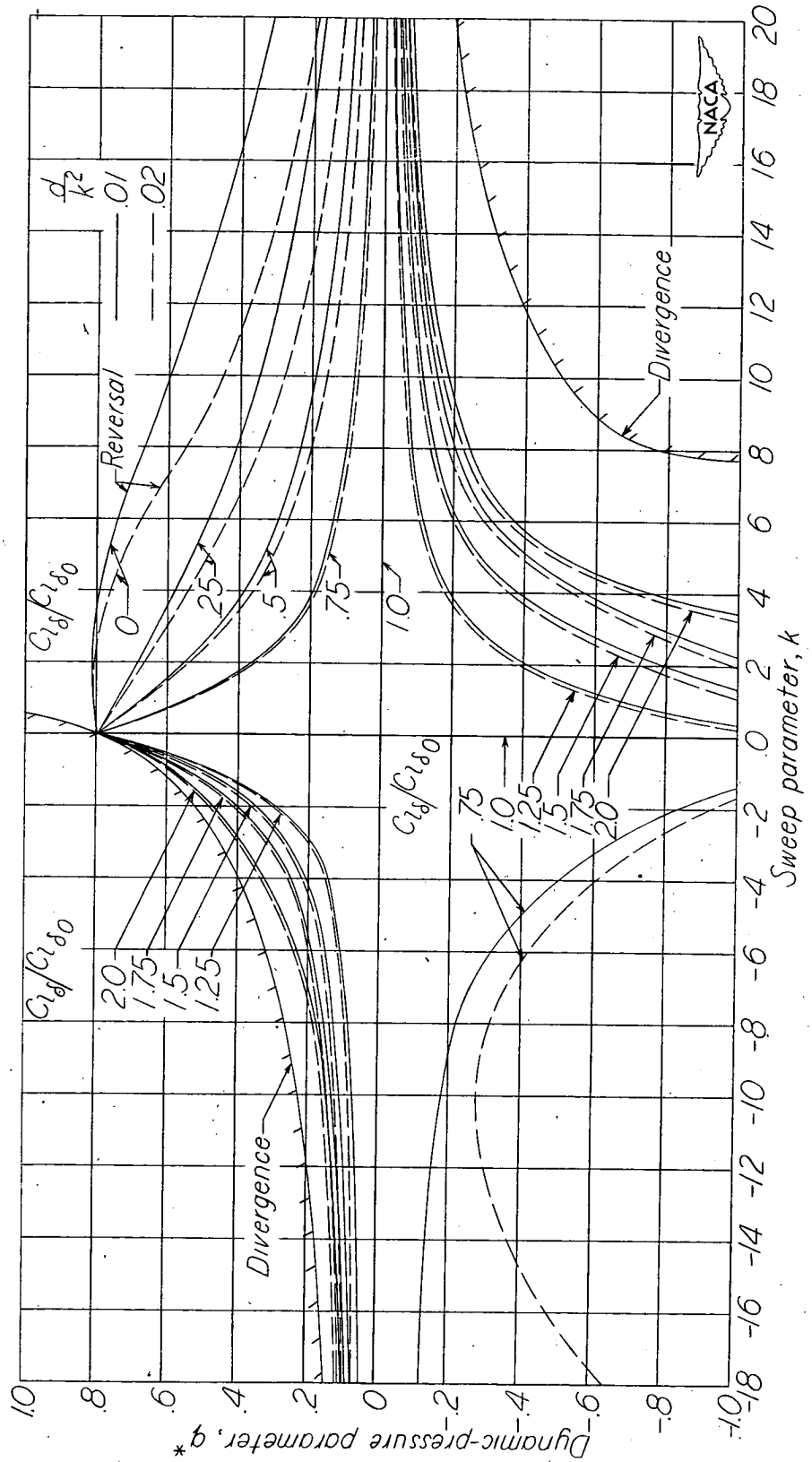

(a) Wings with moment arm $e_2 = 0$.

Figure 5.- Charts for a preliminary survey of lateral control for flexible wings of taper ratio 1.0.

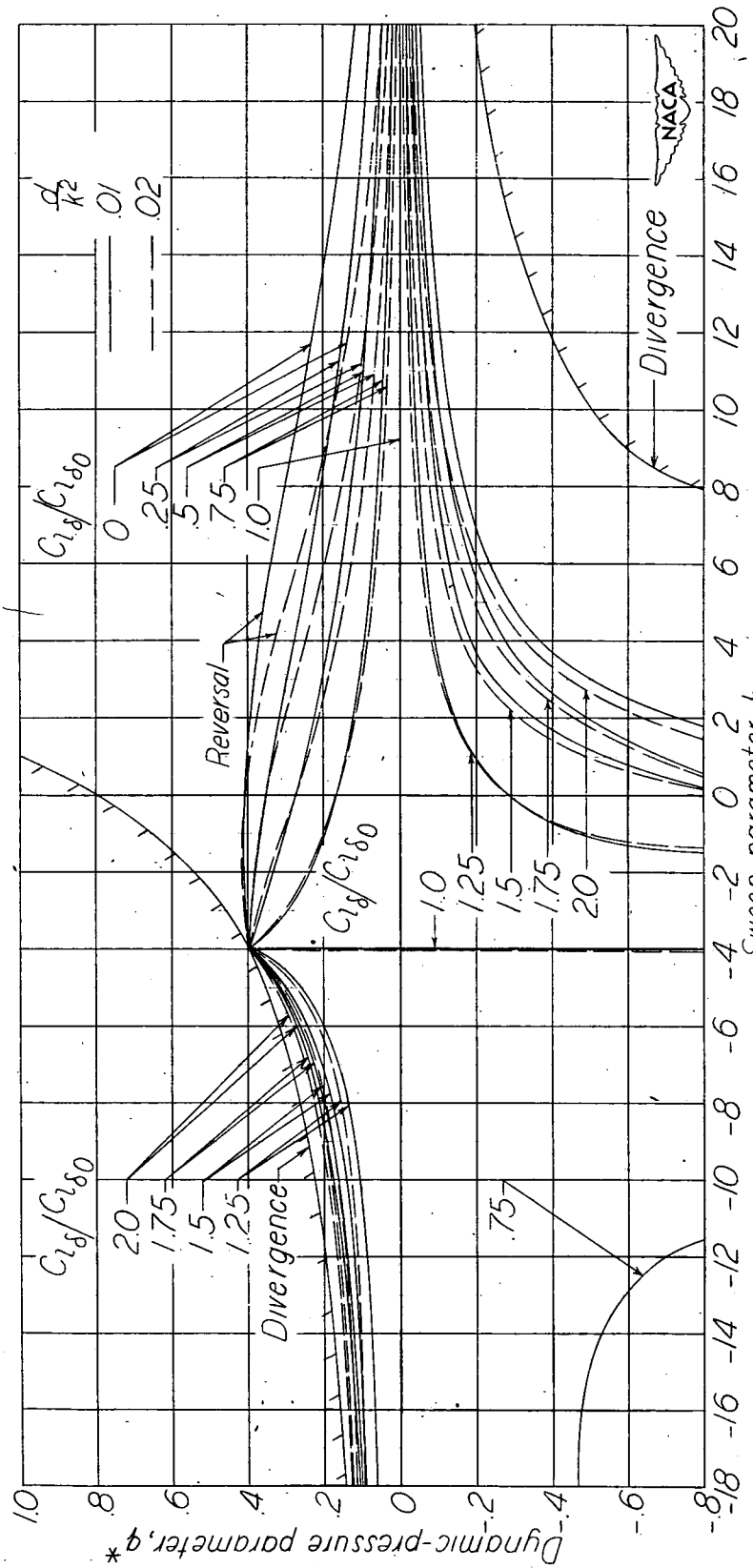

(b) Wings with moment-arm ratio $\epsilon = 1.0$.

Figure 5.- Continued.

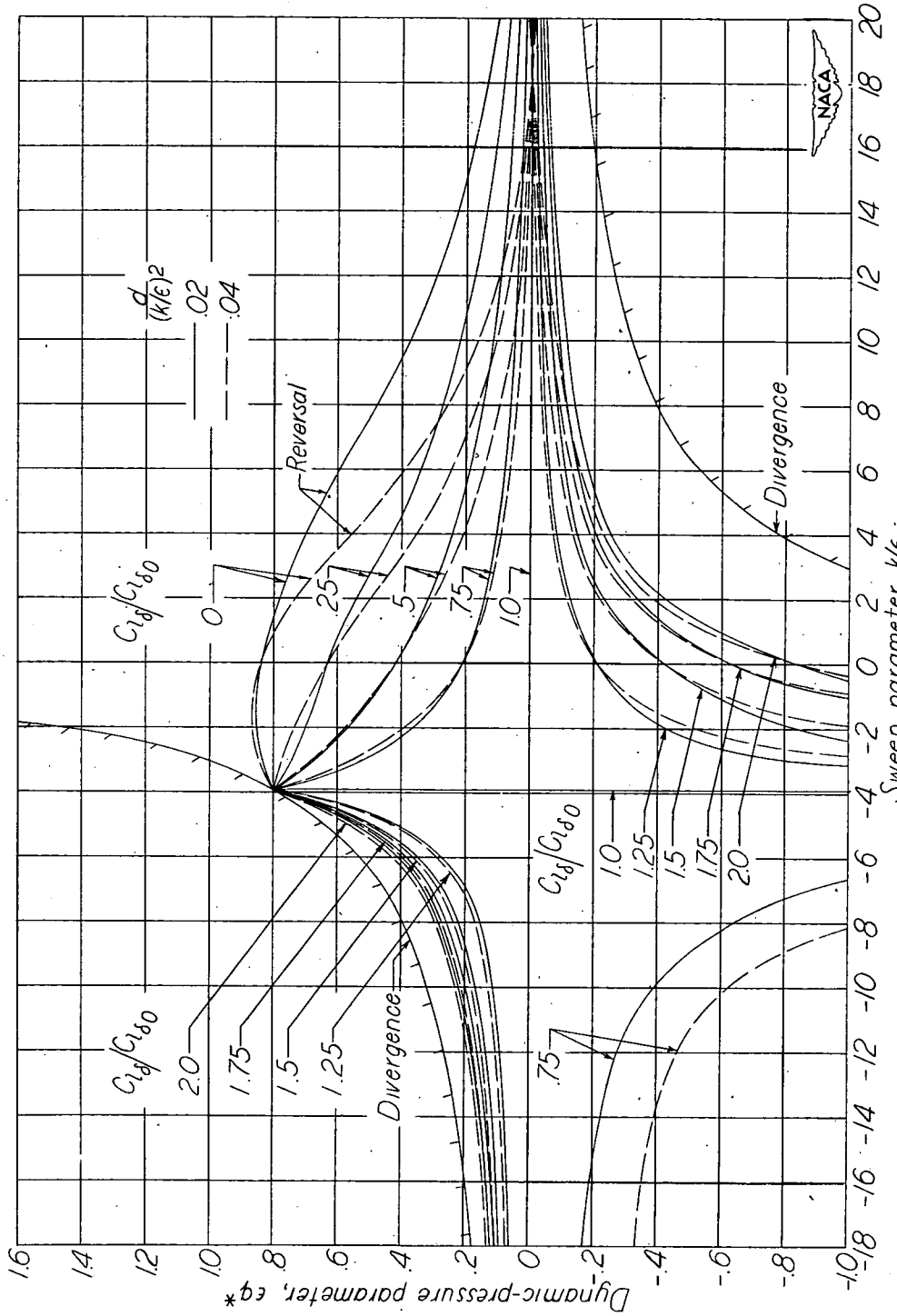

(c) Wings with moment arm $e_1 = 0$.

Figure 5.- Concluded.

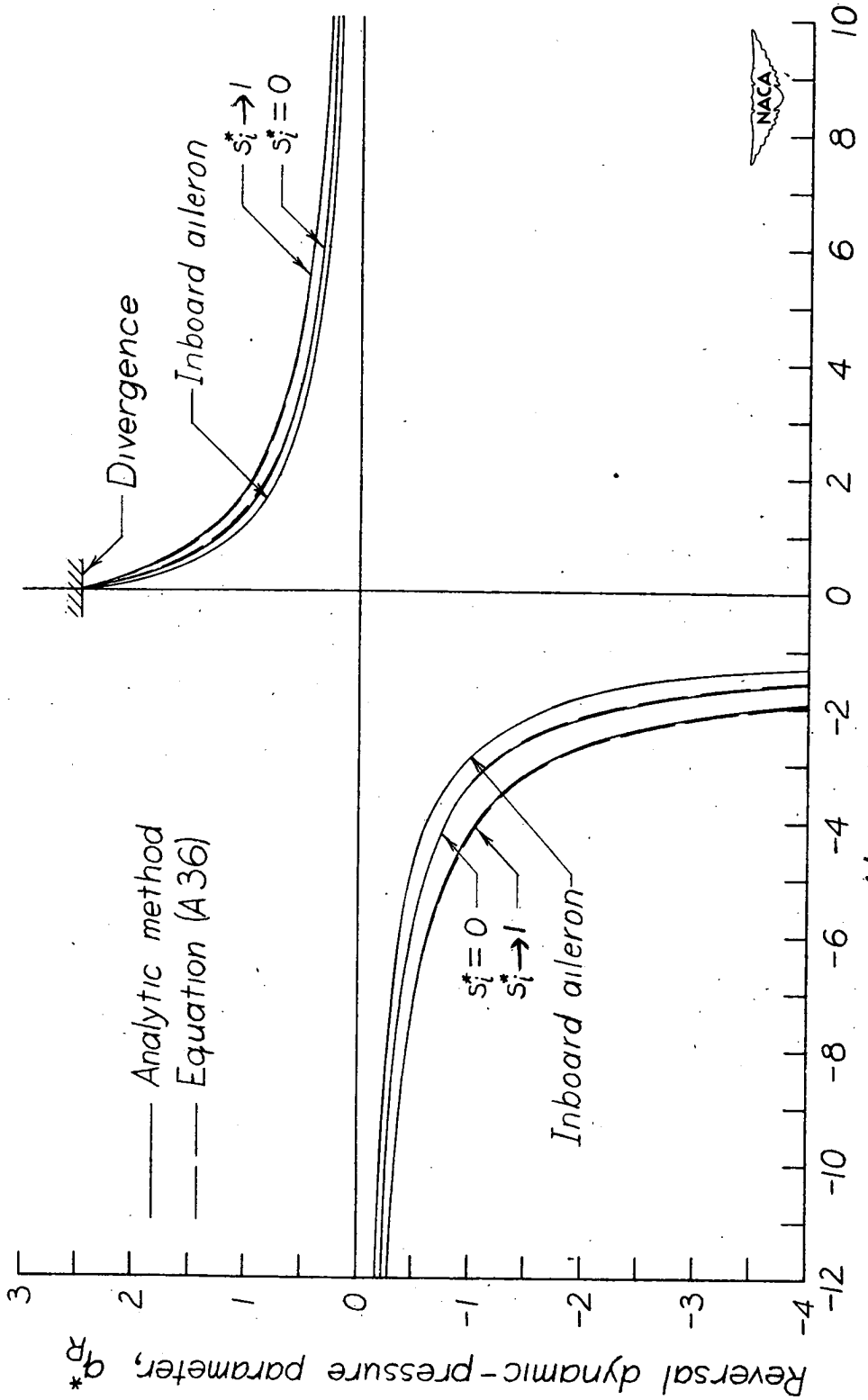

Figure 6.- Comparison of dynamic pressures at aileron reversal calculated by the analytic integration method of the appendix with those calculated from equation (A36) for unswept uniform wings.

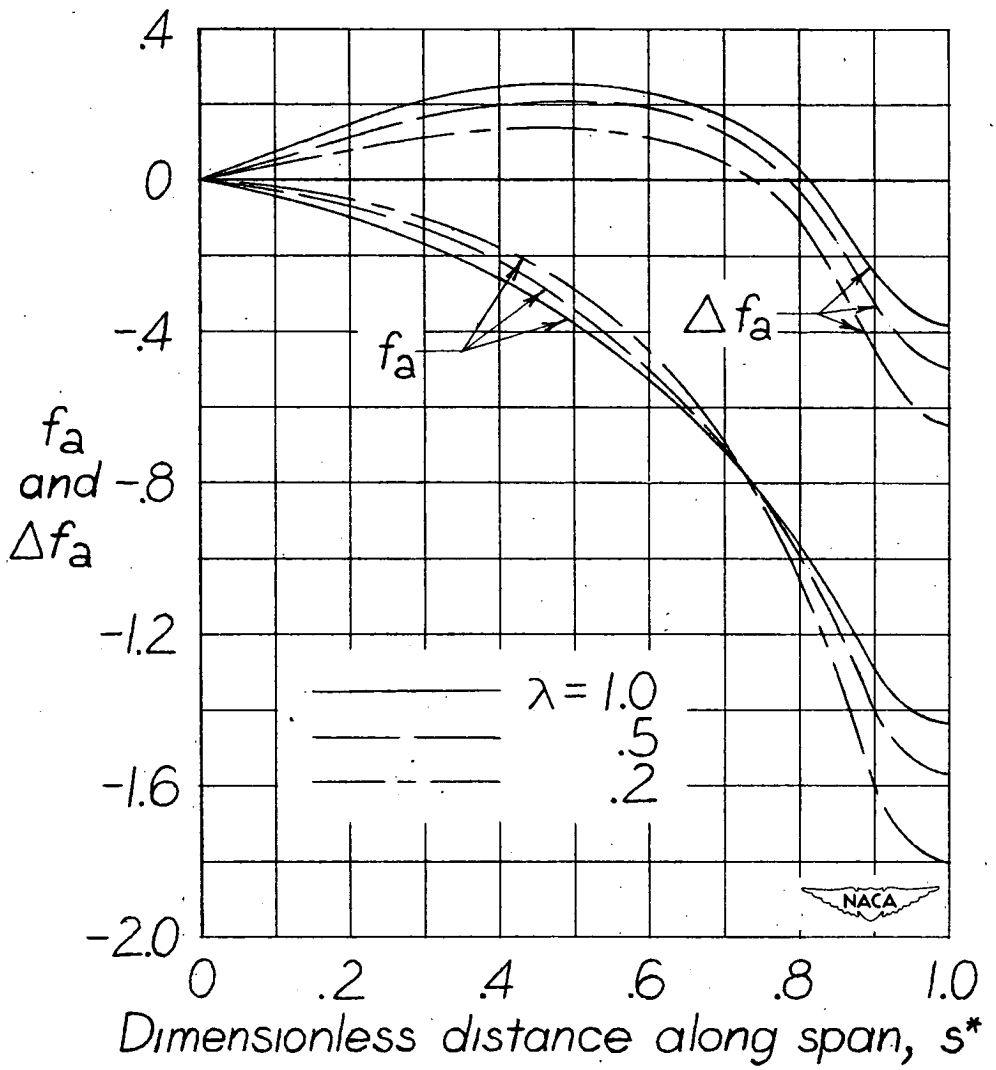

(a) Stiffnesses given by constant-stress criterion for $\frac{(h/c)_t}{(h/c)_r} = 1.0$.

Figure 7.- The angle-of-attack distribution functions f_a and Δf_a for aileron deflections. $s^*_i = 0.5$.

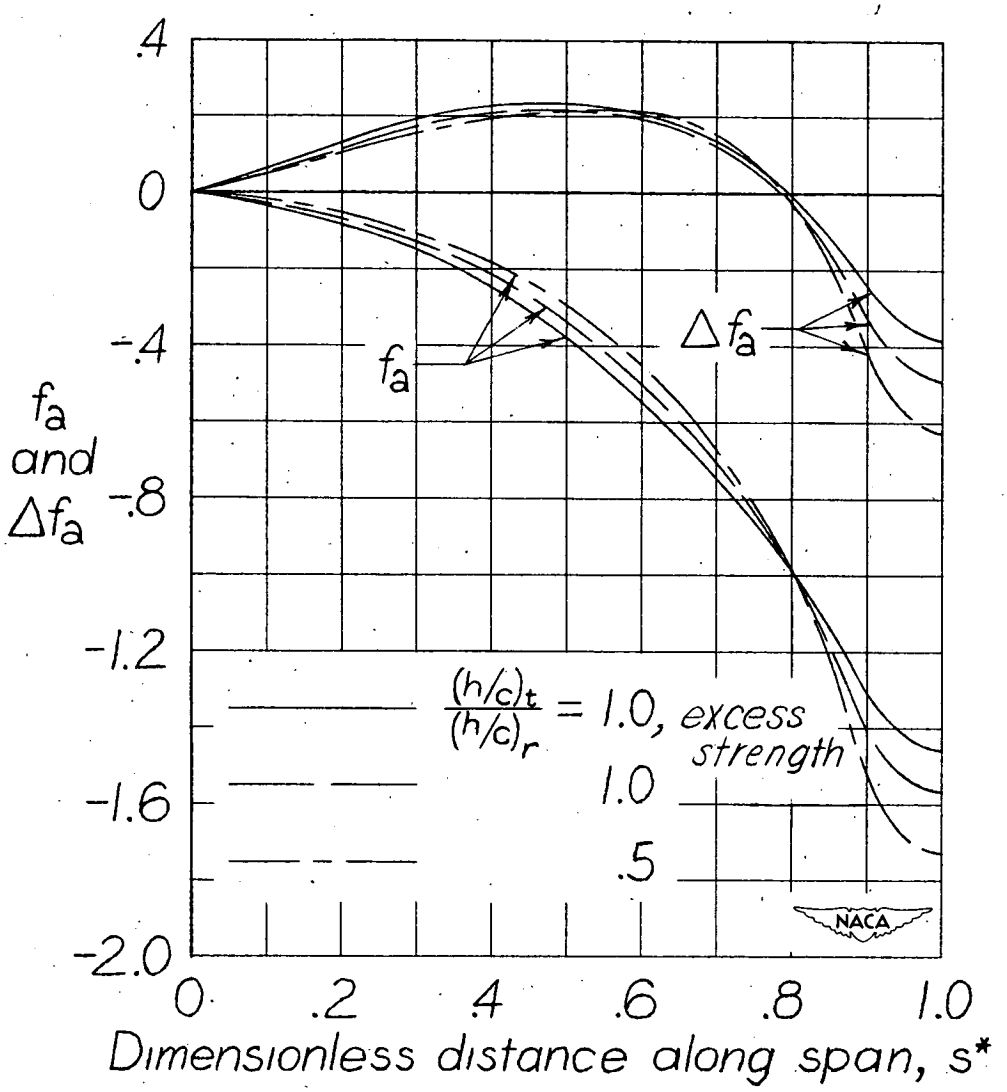

(b) Stiffnesses related to those given by constant-stress criterion for wings of taper ratio 0.5.

Figure 7.- Continued.

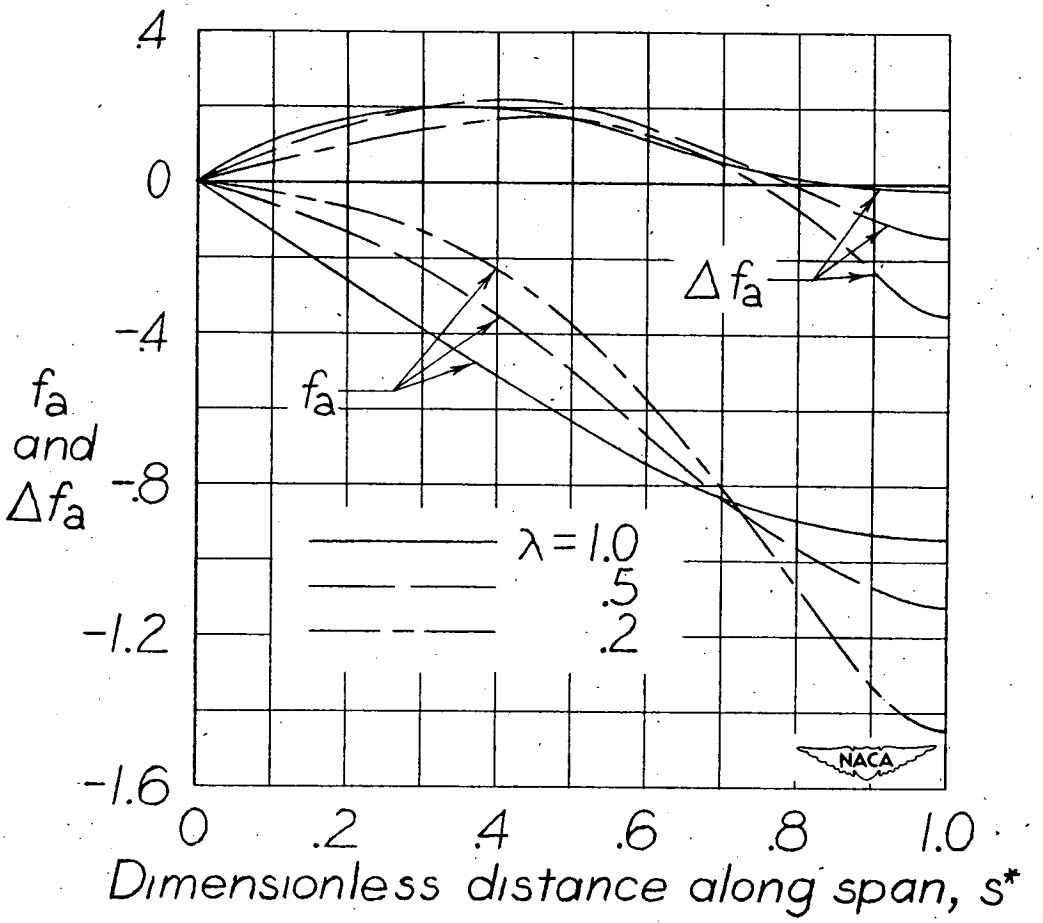

(c) Stiffnesses proportional to c^4.

Figure 7.- Concluded.

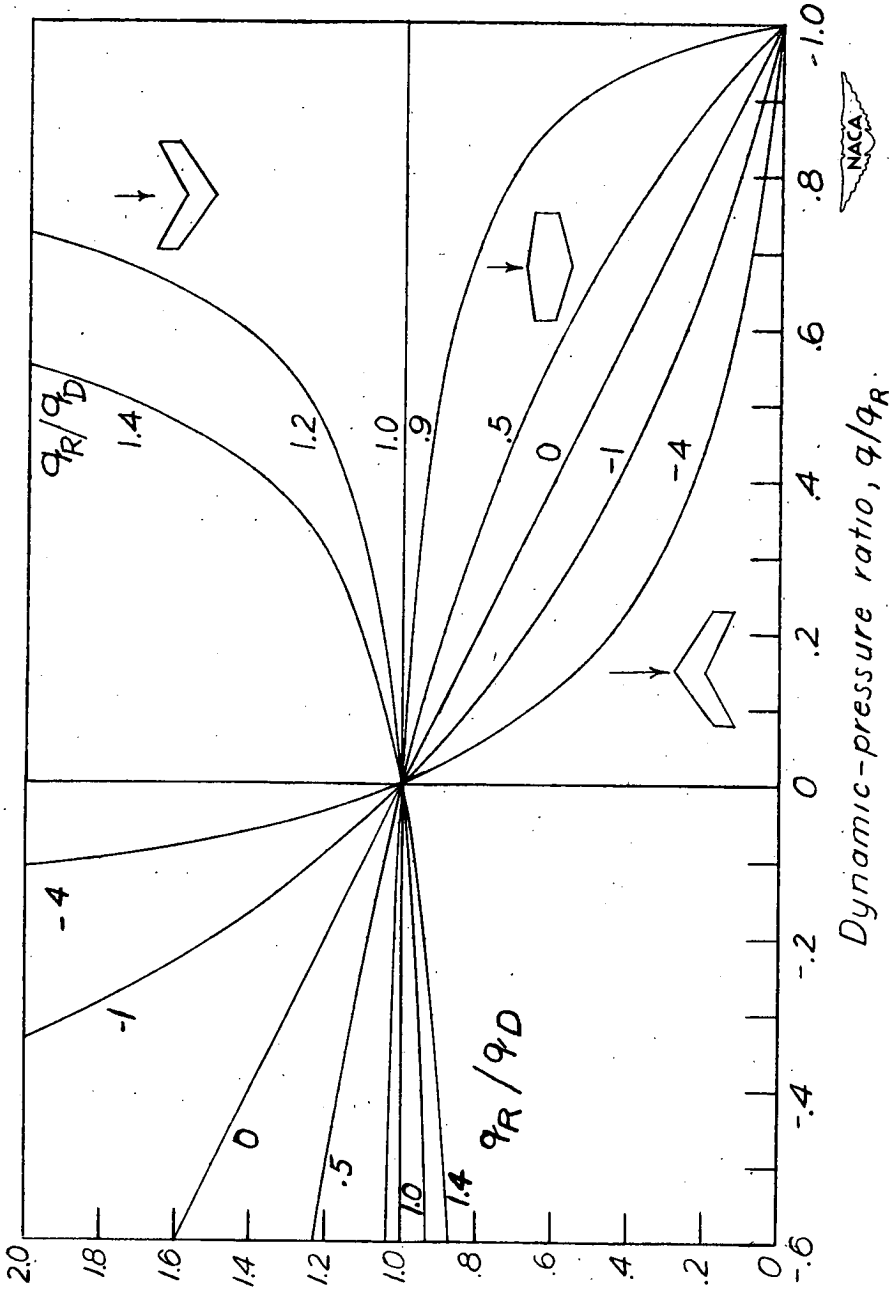

Figure 8.- Variation of aileron rolling effectiveness with dynamic-pressure ratio and the parameter q_R/q_D.

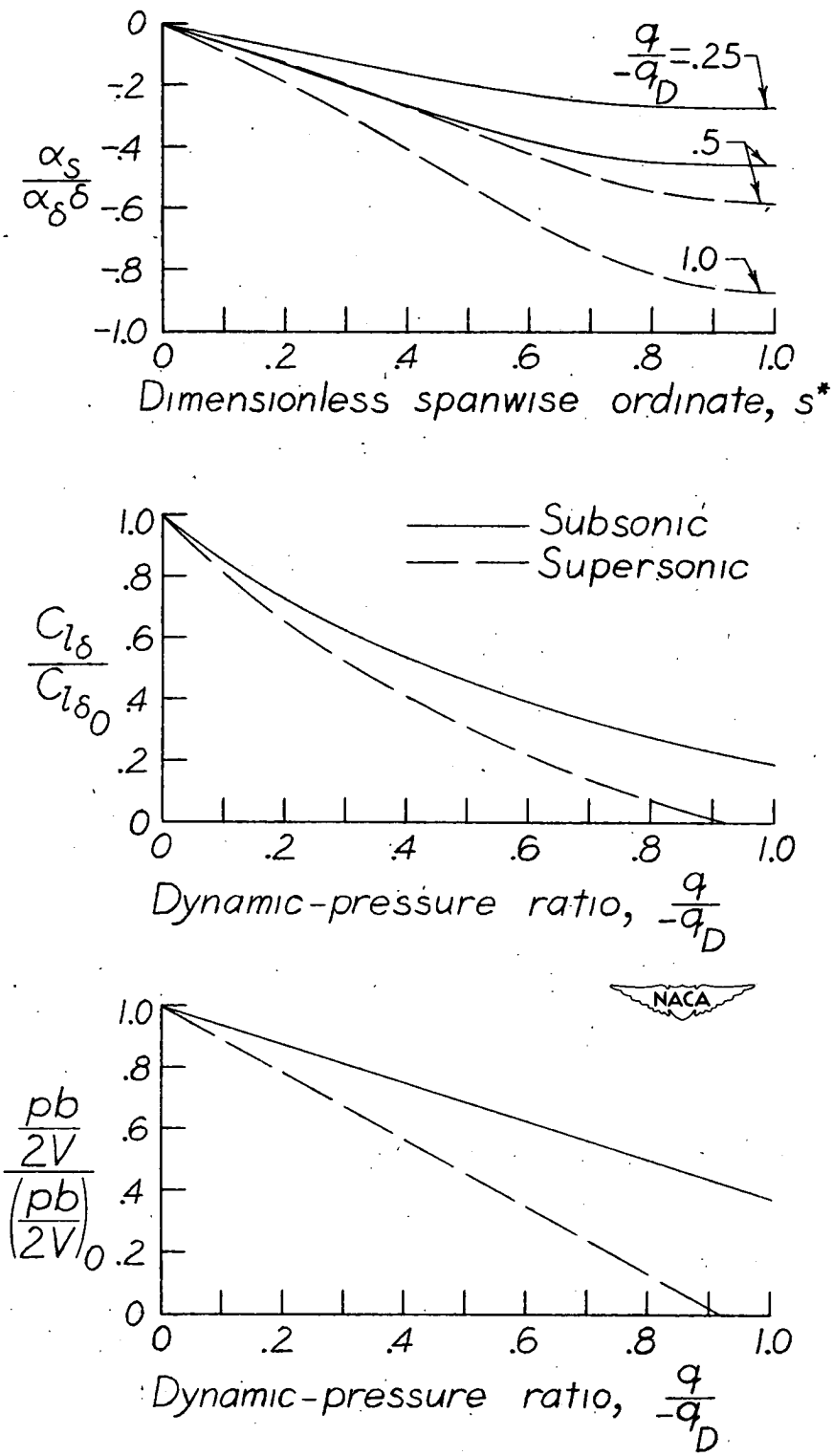

Figure 9.- Effect of aeroelastic action on some lateral-control properties of the example wing.

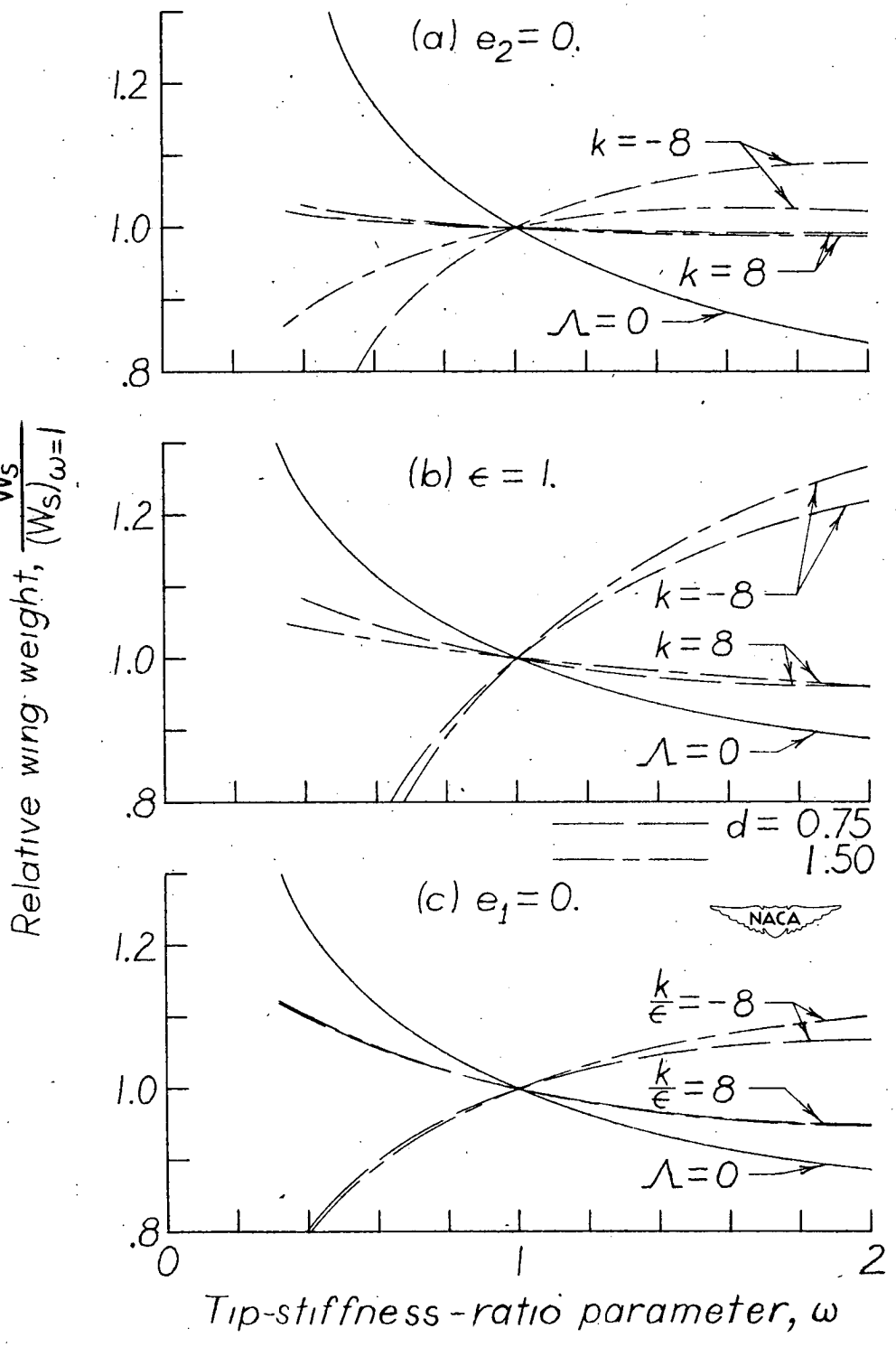

Figure 10.- The effect of tip-stiffness-ratio parameter on the structural weight required to maintain a constant level of lateral-control effectiveness $\left(C_{l_\delta} = 0.8C_{l_{\delta_0}}\right)$ at a given dynamic pressure.

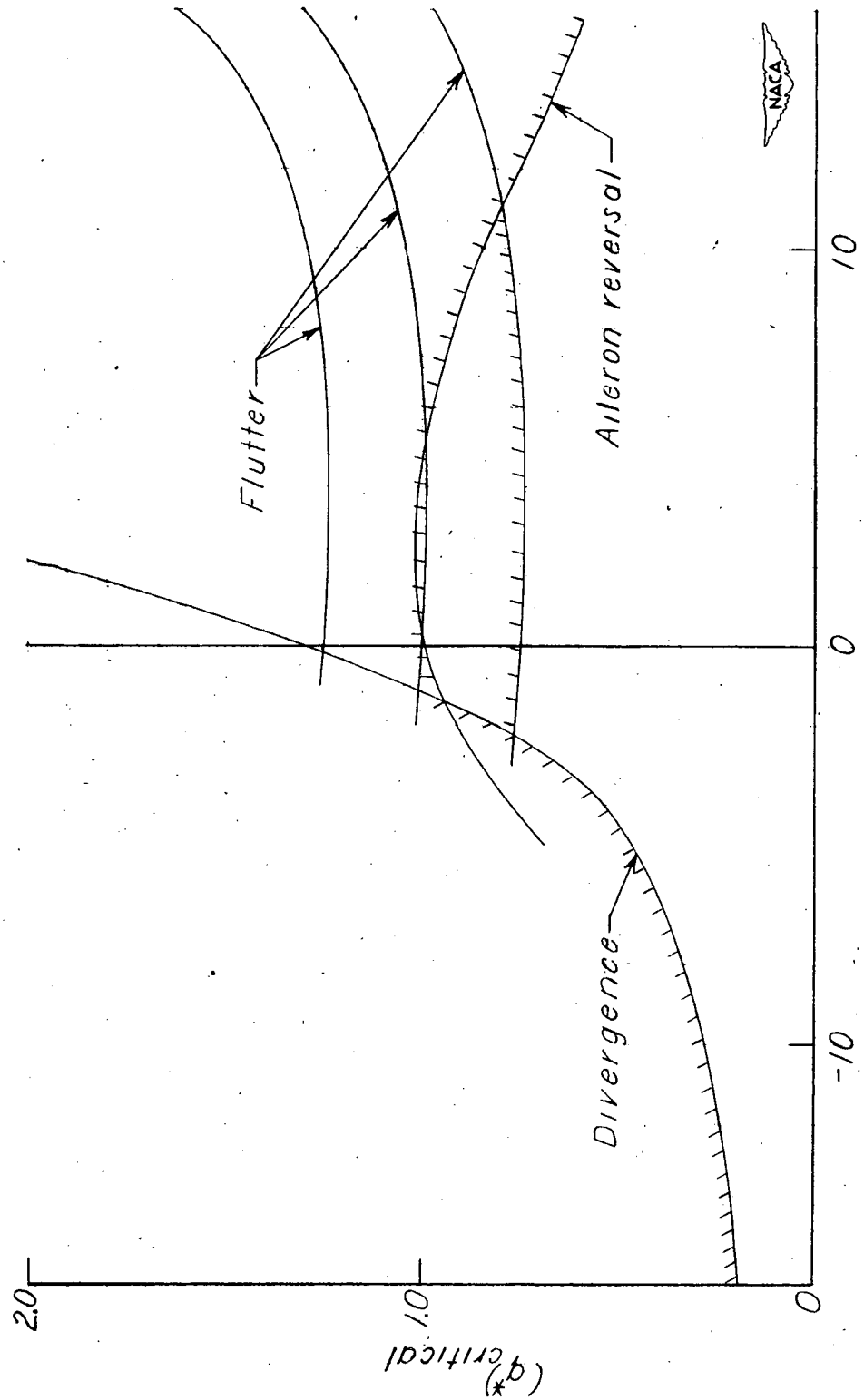

Figure 11.- Variation of critical dynamic pressures with the sweep parameter k.

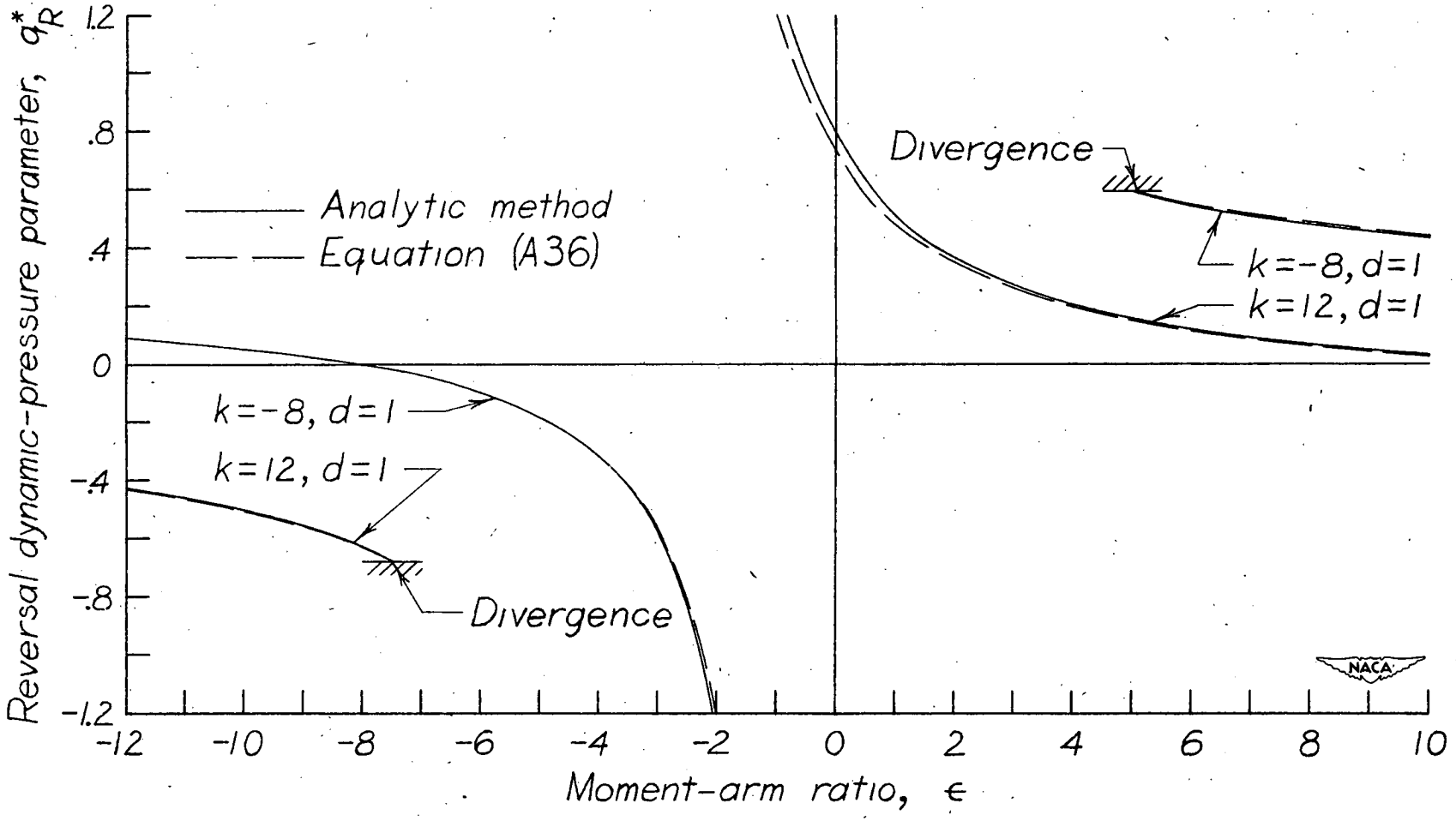

Figure 12.- Comparison of dynamic pressures at aileron reversal calculated by the analytic integration method of the appendix with those calculated from equation (A36) for swept uniform wings with tip ailerons. $s^*_i \rightarrow 1$.

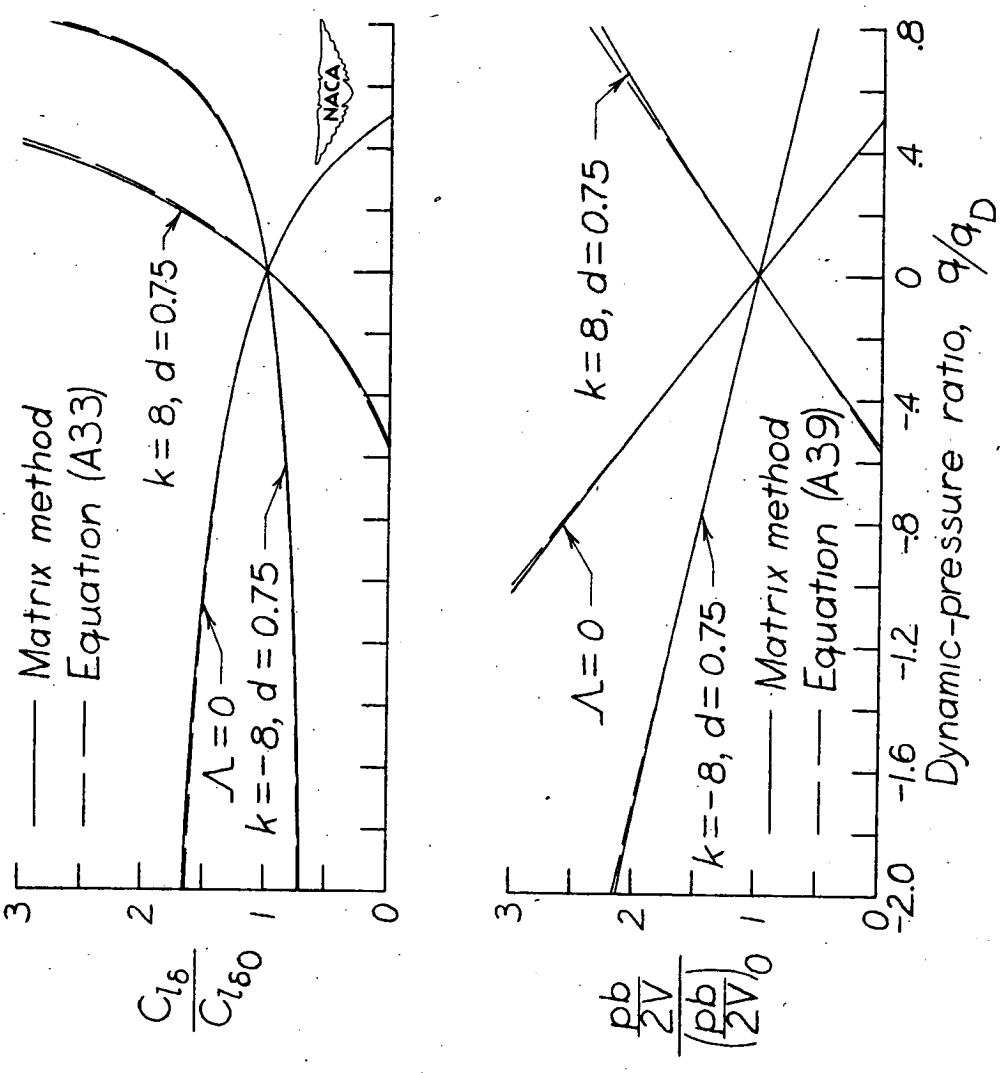

Figure 13.- Comparison of rolling power and rolling maneuverability calculated by the matrix method of the appendix with those calculated by equations (A33) and (A39) for uniform wings. $s^*_i = 0.5$; $\epsilon = 1.0$.

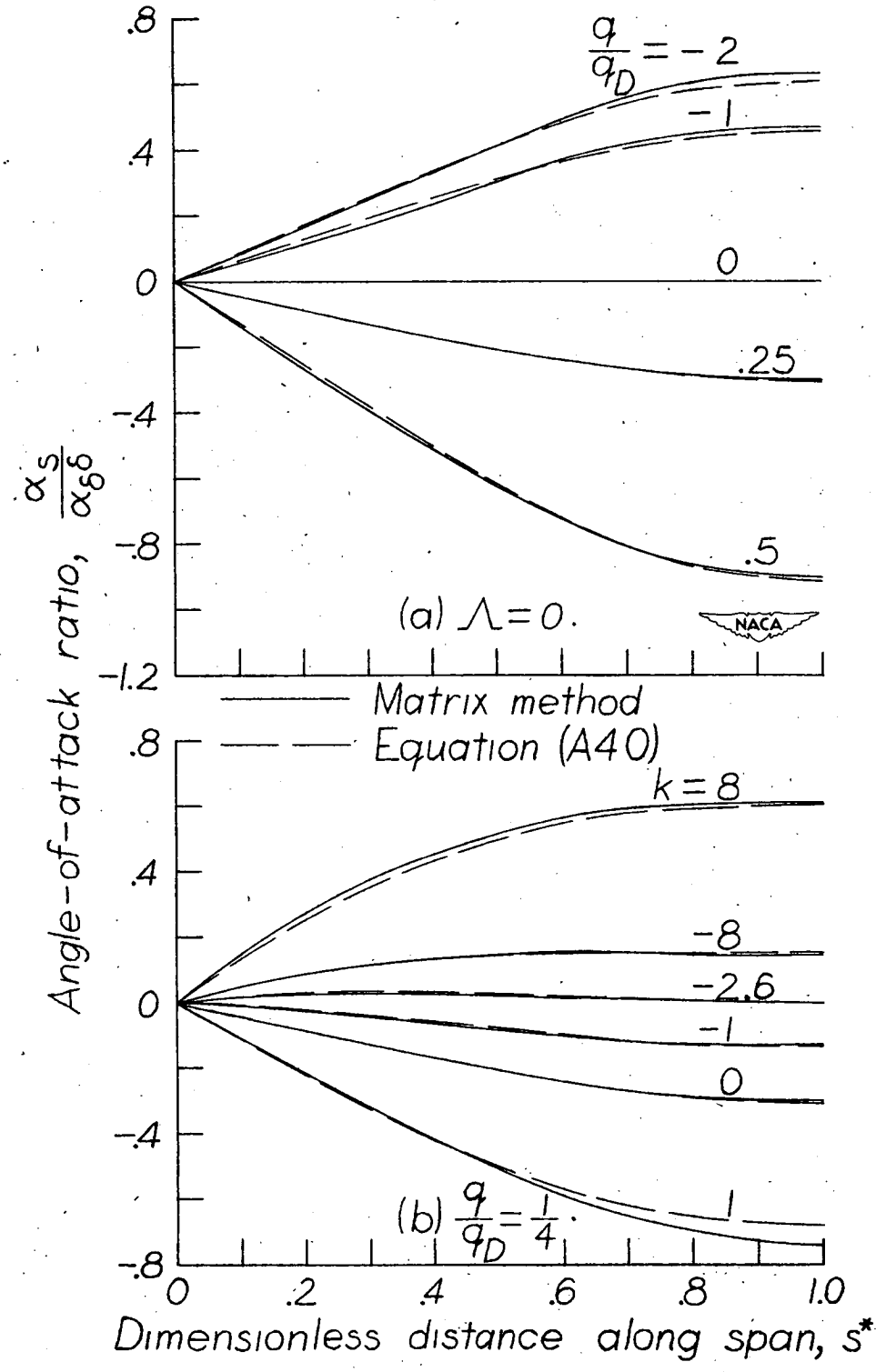

Figure 14.- Comparison of angle-of-attack ratios calculated by the matrix method of the appendix with those calculated by equation (A40) for uniform wings. $s^*_i = 0.5$; $\epsilon = 1.0$.

NACA-Langley.- 7-30-52 - 1000